NACA TN 2240

NATIONAL ADVISORY COMMITTEE FOR AERONAUTICS

TECHNICAL NOTE 2240

THE EFFECT OF NONUNIFORM TEMPERATURE DISTRIBUTIONS ON THE STRESSES AND DISTORTIONS OF STIFFENED-SHELL STRUCTURES

By Richard R. Heldenfels

Langley Aeronautical Laboratory
Langley Air Force Base, Va.

Washington
November 1950

NATIONAL ADVISORY COMMITTEE FOR AERONAUTICS

TECHNICAL NOTE 2240

THE EFFECT OF NONUNIFORM TEMPERATURE DISTRIBUTIONS ON THE STRESSES AND DISTORTIONS OF STIFFENED-SHELL STRUCTURES

By Richard R. Heldenfels

SUMMARY

The structural effects of nonuniform temperature distributions, such as those produced by aerodynamic heating or thermal ice-prevention systems, are discussed and found to be of two types: The introduction of thermal stresses and distortions as a result of restrained thermal expansion and a change in the stresses and distortions produced by the applied loads as a result of the variation of elastic properties of materials with temperature. These effects are illustrated by sample analyses of the stress and distortion distributions of simple box beams and by calculation of the stresses on a typical wing section.

INTRODUCTION

The determination of the structural effects of nonuniform temperature distributions, such as those produced by aerodynamic heating or thermal ice-prevention systems, is rapidly becoming a problem of interest to aircraft designers. Uniform temperature distributions have relatively simple structural effects, but the temperature gradients of nonuniform distributions, which often occur, have important and complex effects on the stresses and distortions of the structure, and their prediction requires the development of analytical methods.

The first step in a thermoelastic analysis is the determination of the temperature distribution, a problem which has received much attention in the recent literature as indicated by the theoretical and experimental work reported in references 1 to 5. The temperature distributions of greatest structural importance are often transitory and their determination requires the simultaneous solution of aerodynamic and heat equations as a function of time. This problem, however, lies beyond the scope of the present paper, which is concerned with the structural effects of a given temperature distribution, and hence all temperature distributions used in the examples have been chosen arbitrarily.

The calculation of the stresses due to various temperature distributions has been treated to some extent by several investigators, since the problem has long been of concern to power-plant and engine designers (for example, see reference 6). The basic concepts are outlined in reference 7 and some specific problems involving simple structures are solved in references 7 and 8; however, the only known work directly related to aircraft structures is the experimental data of reference 9. The required methods that would be directly applicable to the thermoelastic analysis of aircraft structures, therefore, have not as yet been developed.

In the present paper, the effects of temperature changes on aircraft structures are discussed and the various stress and distortion changes are illustrated by several analyses of simplified structures. The analytical methods used are derived in the appendixes and provide relatively simple means of approximating the stresses in complicated structures. A generalized type of analysis, presented in reference 10, yields more accurate results for these cases but requires a much larger amount of work.

THE STRUCTURAL EFFECTS OF TEMPERATURE CHANGES

When an unrestrained isotropic body is heated uniformly, it experiences a uniform expansion that proceeds freely in all directions. If the temperature varies throughout the body, however, each element will try to expand a different amount. Such an expansion cannot, in general, take place freely, and the internal restraint against the expansion will induce thermal stresses in the body. Thermal stresses may similarly be induced by any type of temperature change if the body is externally restrained. These thermal stresses and distortions may be called the thermal-expansion effects of temperature changes.

A change in the temperature of a body also causes a change in its elastic properties, such as the modulus of elasticity, modulus of rigidity, and coefficient of thermal expansion, which have heretofore been considered constant. (For example, see fig. 1, which was compiled from the data of references 11 and 12.) If the entire body is heated uniformly, the elastic properties will change, but they will be constant throughout the body. If the temperature distribution is nonuniform, however, the body will have different elastic properties from point to point and thus will behave differently under an applied load than if the properties were uniform. In each case the effective structure is changed, and the resulting changes in the stresses and distortions may be called the elastic-property effects of temperature changes.

Thus, a structure under an externally applied load and subjected to nonuniform heating will experience a change in the stresses produced by the load plus the addition of thermal stresses. These stress changes are more easily understood if the changes in the component parts of the total stress are studied. In each case the type of stress (load or thermal) is subdivided into elementary and secondary stress components.

The elementary stresses produced by the applied load are determined from the ordinary engineering theory of shell structures which yields the familiar formulas for normal and shear stresses: P/A, Mc/I, VQ/It, and Torque/2At. Secondary stresses appear when the assumptions of elementary theory are not completely valid; for instance the restrained root warping of shell structure results in shear-lag stresses and bending stresses due to torsion. These self-equilibrating secondary distributions are statically indeterminate; thus their calculation is somewhat more complicated than the elementary solutions. The methods usually used for calculation of either elementary or secondary stresses in shells are based on the assumption of constant elastic properties and should therefore be redeveloped on the basis of variable elastic properties if that type of temperature effect is to be calculated accurately.

Methods for determining thermal stresses are not so well established as those for determining stresses due to external loads, but similar considerations can be used to differentiate between elementary and secondary thermal stresses. Secondary stresses again appear when the cross section warps, for instance, near the end of a cantilever beam having a tip cross section that must be free of thermal stress. Thermal stresses are independent of the applied loads; therefore, each stress component is a self-equilibrating system, the magnitude of which depends only upon the temperature distribution and the characteristics of the structure. The changes in elastic properties with temperature also affect the thermal stresses induced by a given temperature gradient, and provision should be made for these effects in the analytical methods developed.

All the changes in the stresses and distortions (load or thermal) of a shell structure caused by temperature changes can be determined by application of the theory of elasticity (for example, see reference 7), provided the elastic properties of the material are known for all temperatures involved. Because of the variation of elastic properties, exact solutions of even the simplest problems are difficult to obtain. In all practical cases simplifying assumptions must be introduced and approximate methods must be used. Several methods for the analysis of simplified structures are developed in the appendixes. In the next section these methods are applied to several problems that illustrate the previously described effects of temperature changes and indicate the relative importance of these effects. In addition, the validity of some simplifying assumptions (constant elastic properties and infinite transverse stiffness) are examined.

ILLUSTRATIVE EXAMPLES

The following examples are presented to illustrate the effects of temperature changes on a shell structure. In order to facilitate the analysis, only very simplified structures are considered, the idealized shell consisting of a number of longitudinal elements that are assumed to carry only axial load and panels, or elements of sheet, that carry only shear. This type of simplified structure is commonly used for the analysis of stiffened shells.

All structures are assumed to be constructed of 75S-T6 aluminum alloy which has the elastic properties shown in figure 1. The symbols used are defined in appendix A, and the equations required for the analysis of these structures are derived in appendixes B to F.

The temperatures used are measured from the temperature at which there is no thermal stress in the structure, which is assumed to be 60° F in the present paper. Thus, in figure 1 and in all the examples $T = 0^\circ$ F corresponds to 60° F.

The possibility of skin buckling is not considered in the following examples. It is apparent from the magnitude of the calculated stresses that buckling occurs in many cases and thus reduces the effectiveness of the skin. Since this factor may be important in design, the effectiveness of the buckled skin at its actual temperature must be determined in practical applications. Reference 11 presents the results of an experimental investigation of compressive buckling of plates at elevated temperatures.

Stress Distribution in a Box Beam

The first series of examples is concerned with the effect of temperature changes on the stress distribution in the box beam shown in figure 2. The box beam is of doubly symmetrical, rectangular cross section and consists of two vertical spar webs, four corner flanges, and a central stringer in each of the covers. It is subjected to a concentrated, vertical tip load of 10,000 pounds. In addition to illustrating the general effects of a temperature change, these examples also are used to demonstrate the significance of variable elastic properties and finite rib stiffness.

General effects of temperature changes.- Figure 3 shows the stress distribution obtained from three different temperature distributions that vary only in the chordwise direction. (The plotted values were determined from the equations derived in appendix B under the assumptions that the box beam has closely spaced rigid ribs, that the temperature is

symmetrical chordwise but invariant spanwise and depthwise, and that the elastic properties vary with temperature.)

Example 1 (fig. 3) shows the distribution of cover shear stress and flange and stringer normal stress when the box beam is at a uniform temperature ($T = 0^\circ$ F) and no thermal stresses are present. The curves merely show the effect of shear lag on the elementary stresses given by ordinary beam theory (Mc/I and VQ/It).

Example 2 (fig. 3) shows the stresses for a case in which the flanges are hotter than the central stringer ($T_F = 250^\circ$ F; $T_S = 125^\circ$ F). A substantial change in the shape of the stress distribution as well as in the magnitude of the stresses is apparent. The maximum normal stress (lower flanges) has increased 24 percent and the maximum shear stress (upper surface) has increased 151 percent over the maximum stresses given in example 1.

Example 3 (fig. 3) presents similar results for a case in which the central stringer is hotter than the flanges ($T_F = 125^\circ$ F; $T_S = 250^\circ$ F). The changes are very similar to those of example 2 but are in the opposite direction and of a slightly different magnitude, the maximum normal stress (upper flanges) increasing 30 percent and the maximum shear stress (lower surface) 142 percent over the maximum values of example 1.

The stress changes illustrated are the result of the two effects of temperature previously described, that is, thermal stresses and varying elastic properties. The changes of stress in the upper and lower stringers are interchanged in examples 2 and 3 because the temperature gradients are interchanged. The changes are of unequal magnitude because the changes in elastic properties lead to a different effective structure in each case. These differences can be examined more closely by considering the changes in each stress component shown in figure 4.

The components of the normal stress in the upper flanges and the shear stresses in the upper surface are shown in figure 4 for each of the three temperature distributions previously considered. The sum of these stress components yields the total stress for these elements plotted in figure 3. The elementary stresses due to the vertical load show changes of about 5 percent because of the changes in the effective structure. These stresses were computed by modifying the well-known formulas Mc/I and VQ/It to include the effect of a variable modulus of elasticity. The shear-lag stresses show a change of approximately 5 percent of the shear-lag stresses for the uniform temperature; this change, however, amounts to less than 1 percent of the elementary stress for the uniform temperature.

The largest changes in the stresses result from the thermal stresses. No thermal stresses were present when the box beam was at a uniform temperature, but the nonuniform distributions introduced thermal stresses amounting to 26 percent of the maximum normal stresses and 146 percent of the maximum shear stresses of the box beam at a uniform temperature. In figure 4, the total thermal stress is given by the solid lines; the elementary thermal stress in the flanges is given by the dashed line; and the difference between that and the total stress is the secondary thermal stress that results from the requirement of zero stress at the end of the beam. All the shear stresses result from the secondary distribution.

The thermal-stress components for the temperatures in examples 2 and 3 are equal and opposite. This result is caused by the particular relationships existing between the stringer and flange areas of the structure analyzed and the fact that the temperature gradients across the beam were equal and opposite in the two examples.

Significance of variable elastic properties.- In the preceding example, the variation of elastic properties with temperature was seen to have a small effect on the stress distribution. However, these changes may be of greater importance for other temperatures, as shown in figure 5. A wide range of flange and stringer temperatures is considered, but the restriction is made that the flange is hotter than the stringer and that the temperature does not vary along the span or across the depth of the box beam. Three components of the flange stress are illustrated as follows:

Figure 5(a) shows the magnitude of the maximum elementary normal or bending stress as a function of flange and stringer temperature. The stress changes are seen to be quite large at the higher temperatures where the modulus of elasticity is changing rapidly.

Figure 5(b) shows the magnitude of the maximum shear-lag stresses, which are largest under conditions that produce the greatest change in the elementary stresses. The change, however, is the reverse of that of figure 5(a) and is of smaller magnitude; thus, the change of elementary stress is somewhat offset.

Figure 5(c) shows the magnitude of the elementary thermal stress as a function of flange and stringer temperatures. Two types of curves are given: The dashed lines represent thermal stresses computed with constant elastic properties (corresponding to $T = 0^{\circ}$ F); whereas the solid lines represent values computed with variable elastic properties. The changing elastic properties have a small effect in the low temperature range because the decrease in the modulus of elasticity is offset by the increase in the coefficient of thermal expansion; however, at higher temperatures the decreasing modulus predominates and large effects

appear. Note that in the upper right-hand portion of the figure some part of the structure will be in the plastic range. The plotted curves which are based on an elastic material are inaccurate in that region.

The effect of variable elastic properties is thus important in many cases. In other instances, however, this effect can be safely neglected, for example, in the computation of shear-lag and thermal stresses in the previous example when $T < 300^{\circ}$ F.

Effects of rib flexibility.- The assumption of closely spaced rigid ribs used in the previous section is a common one in shell analysis. It usually yields good results when the primary stresses act in only one direction. In problems involving nonuniform temperature distributions, however, it might be less valid because spanwise variations in the temperature distribution will induce thermal stresses in the ribs. The following examples illustrate the effects of such transverse loading.

The box beam in figure 2 was divided into 5 equal bays by ribs having an effective cross-sectional area equal to that of the flange and was analyzed by the methods developed in appendix C. The results of the analysis are shown in figure 6. Figure 6(a) gives the four assumed temperature distributions, each of which is constant across the depth of the box beam. Example 1 is a case of uniform temperature distribution of $T = 0^{\circ}$ F; example 2 introduces a chordwise gradient that does not vary spanwise; and examples 3 and 4 add linear variations in the spanwise direction. Figures 6(b) and 6(c) give the distributions of normal stress for each of the four cases, the former for temperature distributions in which the flange is hotter than the stringer and the latter for the reverse conditions.

For the structure with the uniform temperature (example 1) the effect of rib flexibility is so small that it cannot be shown in figure 6 to the scale used. A similar result is obtained in example 2, in which there is no spanwise variation of temperatures. However, the two examples of linear spanwise variation (examples 3 and 4) show a small difference of about 3 percent in the total stress. This small difference in the total stress is rather insignificant for this specific example but may be larger in other problems. A closer examination of the various stress components reveals that most of the change is associated with the thermal stresses. Figure 7 shows the magnitude of the thermal-stress component for examples 2, 3, and 4. The assumption of rigid ribs can be seen to lead to an error of about 1,000 psi in examples 3 and 4, which have a spanwise temperature variation. In example 3 this error was 18 percent of the maximum thermal stress.

Rib flexibility is therefore seen to have an important effect on the thermal stress distribution. Whenever the temperature distribution has sharp gradients in either the spanwise or depthwise direction, it

should be considered as a possible source of error. Its importance, however, in any specific problem is influenced by many unrelated factors and no general recommendations are possible.

Distortion of a Four-Flange Box Beam

Knowledge of the distortions of an aircraft structure is an essential part of static and dynamic aeroelastic problems that arise in the design of modern high-speed aircraft. The following simple examples are presented to aid in the estimation of the thermal distortions of various structural elements.

The temperature distributions considered in the previous examples were symmetrical across the chord and constant across the depth and, therefore, have only a small effect upon the distortions. Other than extension in the spanwise direction, the increased temperatures change the deflection only because of changes in the elastic properties of the material. The more interesting case is that in which the temperature is not symmetrical with respect to the center lines of the cross section so that the box beam will bend and twist.

The thermal distortions of the four-flange box beam shown in figure 8 are illustrated in figure 9. The box beam is not loaded; all distortions shown result from heating only one flange. Results are presented for three different spanwise distributions of this flange temperature. The method of analysis used was that of appendix D, in which rigid bulkheads and constant elastic properties are assumed. These assumptions introduce small errors that are neglected in order to simplify the analysis.

The results show that in each case the box beam deflects away from the heated flange in both the horizontal and vertical directions. In addition, the box twists a small amount because of cross-sectional warping that results from the spanwise variation of temperature and the end effects due to the stress-free boundary condition at the tip.

Analysis of a Wing Section

The previous examples treated structures that were highly idealized in order to obtain simple, exact solutions which yield good qualitative results for more complicated structures. Such simple cases are often different from the aircraft structures encountered in practice and a method of analysis that can easily be applied is needed. One possibility is the extension of ordinary shell theory to include temperature effects as is done in appendix E. The equations developed are very similar to those usually employed in airplane stress analysis and give an elementary

stress distribution that includes the effects of both applied load and temperature distribution.

Application of this method is illustrated by an analysis of the idealized, circular-arc wing section shown in figure 10(a). The section analyzed is taken some distance from the tip in order that end effects will be negligible. The temperature distribution is assumed constant spanwise but to have the chordwise variation shown in figure 10(b). Figure 10(c) shows the applied moments and forces. The calculations and results are tabulated in table I, which lists section properties, bending stresses, and shear stresses. For purposes of comparison the values of the stresses produced by the load when the structure is at a uniform temperature of $T = 0^{\circ}$ F are also listed.

The results show that the temperature changes alter the normal stress by as much as 15,000 psi; this change is primarily the result of the induced thermal stresses. The largest changes in stress are in the webs which are at a lower temperature than the rest of the structure. The maximum normal stress changed its location from elements 5a, 5b, and 5c on the compression side to element 7a on the tension side and increased in magnitude 16 percent. The increase in the maximum shear stress was about 3 percent. Since the temperature does not vary spanwise, there are no shear stresses due to thermal expansion and all the change in the shear stresses is due to the change in elastic properties. In this example, both the maximum shear and normal stresses would have been underestimated by about 3 percent if the elastic properties had been assumed constant.

In this analysis, the wing section was taken some distance from the tip in order that the end effects could be neglected. In the tip region the shear stress associated with the end effect may be important and some method of determining it is desirable. An exact mathematical analysis similar to that used on the simple box beams becomes exceedingly complex when applied to a structure such as that considered herein. If an accurate solution is desired, a numerical method of analysis (reference 10) has been developed, but this type of analysis often results in extensive and tedious computational procedures. However, a simple means of approximating the solution, such as that developed in appendix F, may be used.

The calculations required to approximate the end effect in a uniform wing with the cross section and temperature distribution of figure 10 are summarized in table I(d) and the shear stresses at the tip are listed. In this example the end effect becomes negligible 75 inches, or 1 chord length of the idealized cross section, from the tip.

CONCLUDING REMARKS

Temperature changes may have important effects upon the strength and distortion of an aircraft structure, and they should be given careful consideration in the design. These effects are of two types: The introduction of thermal stresses and distortions as a result of restrained thermal expansion and a change in the stresses and distortions due to applied loads as a result of the variation of elastic properties of materials with temperature. The relative importance of these two effects depends on several unrelated variables and must be determined for each particular case; the thermal-expansion effect, however, will often be the more important.

These effects can be calculated by modifying accepted methods of stress analysis as is done in the appendixes. The elementary method of analysis will be of greatest practical value since it provides an easy method for calculating the effects of temperature on the elementary stresses, due to both applied load and temperature, in a shell structure of arbitrary shape. However, it is incapable of predicting secondary stresses, which are often important. Secondary stresses can be estimated easily by applying the exact methods of analysis to a simplified model of the structure or by applying the approximate method of analysis to a more complicated model. An accurate determination of secondary stresses in a complicated structure requires methods beyond the scope of this paper.

As in most types of analysis, it is often possible to introduce simplifying assumptions (constant material properties or infinite transverse stiffness) and still obtain satisfactory results. However, these assumptions are often less valid when nonuniform temperature distributions are involved and they must be used with caution.

Langley Aeronautical Laboratory
National Advisory Committee for Aeronautics
Langley Air Force Base, Va., September 14, 1950

APPENDIX A

SYMBOLS

A	cross-sectional area, square inches
a	length of bay, inches
b	width of panel, inches
c	depth of web, inches
E	modulus of elasticity, psi
G	modulus of rigidity, psi
I	moment of inertia, inches^4
K	stiffness parameter
l	length of beam, inches
M	moment, inch-pounds
N	effective moment due to restrained thermal expansion, inch-pounds
P	statically determinate force group, pounds
Q	area moment, inches^3
q	shear flow, pounds per inch
t	thickness, inches
T	temperature increment, measured from temperature of zero thermal stress which is 60° F in all examples considered, degrees Fahrenheit
U	strain energy, inch-pounds
u,v,w	displacements in x-, y-, z-directions, respectively, inches
V	applied vertical load, pounds
X	statically indeterminate force group, pounds

x,y,z	coordinate axes
$\bar{y},\bar{z}$	y- and z-coordinates of centroid, inches
α	coefficient of thermal expansion, inches per inch per degree Fahrenheit
ϵ	normal strain, inches per inch
η	effectiveness factor
θ	angle of twist, radians
σ	normal stress, psi
τ	shear stress, psi
φ	decay function

Subscripts:

b	panel width
c	web depth
F	flange
i,j	specific stations in x- and y-directions, respectively
o	initial or reference value
P	P-force group
R	rib
S	stringer
W	web
X	X-force group
x,y,z	coordinate axes

APPENDIX B

THREE-ELEMENT PANEL WITH CLOSELY SPACED RIGID RIBS

Equations are derived for the analysis of a flat panel loaded by a uniform shear flow along the longitudinal edges. The panel, shown in figure 11, consists of two flanges and a central stringer which carry only axial loads plus two sheets which carry only shear. The assumptions are made that there are closely spaced rigid ribs in the transverse direction and that the cross section and temperature distributions are symmetrical about the longitudinal center line. These assumptions and the following derivation are very similar to those for the single-stringer method of shear-lag analysis (reference 13), the difference being in the introduction of temperature effects.

The stress-strain relations for the flange, stringer, and sheet are, respectively,

$$\sigma_F = E_F\left(\frac{du}{dx} - \alpha T\right)_F \tag{B1}$$

$$\sigma_S = E_S\left(\frac{du}{dx} - \alpha T\right)_S \tag{B2}$$

$$\tau = \frac{G}{b}(u_F - u_S) \tag{B3}$$

The equations of equilibrium for the flange and stringer are, respectively,

$$\frac{d}{dx}(A\sigma)_F - \tau t = -q \tag{B4}$$

$$\frac{d}{dx}(A\sigma)_S + \tau t = 0 \tag{B5}$$

If the assumption is made that the structural dimensions, panel temperature, and applied shear flow are constant in the x-direction, the following differential equation for τ can be obtained by differentiating equation (B3) twice with respect to x and substituting from equations (B1), (B2), (B4), and (B5):

$$\frac{d^2\tau}{dx^2} - K^2\tau = -q\,\frac{G}{b(AE)_F} \tag{B6}$$

where

$$K^2 = \frac{Gt}{b}\left[\frac{1}{(AE)_F} + \frac{1}{(AE)_S}\right]$$

With boundary conditions of zero normal stress at the tip and zero stringer displacement at the root, differential equation (B6) can be solved and the following equations for the stress distribution are obtained:

$$\sigma_F = q\frac{E_F}{(AE)_F + (AE)_S}\left[l - x + \frac{(AE)_S \sinh K(l - x)}{(AE)_F K \cosh Kl}\right] -$$

$$\frac{1}{A_F}\frac{Gt}{K^2 b}\left[(\alpha T)_F - (\alpha T)_S\right]\left(1 - \frac{\cosh Kx}{\cosh Kl}\right) \tag{B7}$$

$$\sigma_S = q\frac{E_S}{(AE)_F + (AE)_S}\left[l - x - \frac{\sinh K(l - x)}{K \cosh Kl}\right] +$$

$$\frac{1}{A_S}\frac{Gt}{K^2 b}\left[(\alpha T)_F - (\alpha T)_S\right]\left(1 - \frac{\cosh Kx}{\cosh Kl}\right) \tag{B8}$$

$$\tau = \frac{q}{t}\,\frac{(AE)_S}{(AE)_F + (AE)_S}\left[1 - \frac{\cosh K(l - x)}{\cosh Kl}\right] +$$

$$\frac{K}{t}\frac{Gt}{K^2 b}\left[(\alpha T)_F - (\alpha T)_S\right]\frac{\sinh Kx}{\cosh Kl} \tag{B9}$$

In equations (B7), (B8), and (B9), each individual term represents a particular stress component. The first group of terms in each equation gives the stresses due to the applied load q and the second group gives the thermal stresses. Each of these groups is in turn made up of an elementary and a secondary stress. The elementary load stresses are equivalent to Mc/I for σ and VQ/It for τ, and the secondary component is a shear-lag stress. The elementary thermal stress does not

produce shear in the sheets; however, the secondary component, due to the end effect, contributes both normal and shear stresses. Observe that all terms contain the elastic properties which vary with temperature.

APPENDIX C

THREE-ELEMENT PANEL WITH FLEXIBLE RIBS

The structure analyzed is similar to that of appendix B except, in this case, the transverse stiffness is provided by individual flexible ribs that divide the structure into a number of bays. Within each bay the properties of the structure, the shear stress, and the temperature distribution are assumed constant. The panel can then be analyzed by the method of reference 14. This method, which is applicable to most shell structures, describes the state of stress in terms of characteristic force groups. For a shell of n elements (or stringers) there are n independent force groups, three of which are statically determinate, the others being statically indeterminate. The magnitude of each group is then determined by minimizing the strain energy of the structure. In complicated cases the analysis may be simplified by using orthogonal force groups.

In the present case, there are three independent force groups for the three-element flat panel being analyzed, but since only symmetrical stress distributions are of interest, only two force groups are required. These two force groups, one equilibrating the external loads and the other self-equilibrating and statically indeterminate, are shown in figure 12, in which the sign conventions and notation employed are also shown.

The force group P_i equilibrates the shear flow applied along the longitudinal edges and can be determined from the following equation of static equilibrium and the boundary conditions on the stresses:

$$q_{W,i} = \frac{2}{a_i}(P_{i-1} - P_i) \tag{C1}$$

The total forces in the flanges and stringer at the ith rib then are

$$P_{F,i} = P_i + X_i \tag{C2a}$$

$$P_{S,i} = 2(P_i - X_i) \tag{C2b}$$

The shear flow in the ith panel produced by each force group is

$$q_{P,i} = \frac{1}{a_i}(P_{i-1} - P_i) \tag{C3a}$$

$$q_{X,i} = \frac{1}{a_i}(X_{i-1} - X_i) \tag{C3b}$$

and the total shear flow is

$$q_i = q_{P,i} - q_{X,i} = \frac{1}{a_i}(X_i - X_{i-1} - P_i + P_{i-1}) \tag{C4}$$

The ribs are loaded by the change in shear between bays and thus the load in the ith rib where it intersects the central stringer is

$$P_{R,i} = b(q_{i+i} - q_i)$$

$$= (X_{i+1} - P_{i+1})\frac{b}{a_{i+1}} - (X_i - P_i)\left(\frac{b}{a_{i+1}} + \frac{b}{a_i}\right) + (X_{i-1} - P_{i-1})\frac{b}{a_i} \tag{C5}$$

Equations (C2), (C3), (C4), and (C5) express all of the internal forces in terms of the known P-forces and unknown X-forces. These unknown forces can be determined by the principle of minimum complementary energy. In writing the expression for the complementary energy, the energy required to change the temperature of the structure must be included. It is most easily accomplished in this case by using the analogy between thermal stresses and body forces (reference 7); then the energy expression is

$$\begin{aligned} U = \sum_i \Bigg\{ & \frac{1}{2}\int_0^{a_i} \frac{2}{(AE)_{F,i}}\left[P_{F,i}\,\frac{x}{a_i} + P_{F,i-1}\left(1 - \frac{x}{a_i}\right)\right]^2 dx + \\ & \frac{1}{2}\int_0^{a_i} \frac{1}{(2AE)_{S,i}}\left[P_{S,i}\,\frac{x}{a_i} + P_{S,i-1}\left(1 - \frac{x}{a_i}\right)\right]^2 dx + \\ & \frac{1}{2}\int_0^{b} \frac{2}{(AE)_{R,i}}\left(P_{R,i}\,\frac{y}{b}\right)^2 dy + 2\frac{1}{2}\,q_i^2\left(\frac{ab}{Gt}\right)_i + \\ & 2\int_0^{a_i} (\alpha T)_{F,i}\left[P_{F,i}\,\frac{x}{a_i} + P_{F,i-1}\left(1 - \frac{x}{a_i}\right)\right] dx + \\ & \int_0^{a_i} (\alpha T)_{S,i}\left[P_{S,i}\,\frac{x}{a_i} + P_{S,i-1}\left(1 - \frac{x}{a_i}\right)\right] dx + \\ & 2\int_0^{b} (\alpha T)_{R,i}\left(P_{R,i}\,\frac{y}{b}\right) dy \Bigg\} \end{aligned} \tag{C6}$$

By minimizing equation (C6) with respect to each unknown X-force group, a system of simultaneous linear equations is obtained. The X-forces can then be determined by solving this set of equations. The general equation obtained from the minimization process can be written as follows:

$$\omega_{i,i-2}X_{i-2} + \omega_{i,i-1}X_{i-1} + \omega_{i,i}X_i + \omega_{i,i+1}X_{i+1} + \omega_{i,i+2}X_{i+2} = \lambda_i \qquad (C7)$$

where

$$\omega_{i,i-2} = \left(\frac{2b^3}{3AE}\right)_{R,i-1} \frac{1}{a_{i-1}} \frac{1}{a_i}$$

$$\omega_{i,i-1} = \left[\left(\frac{a}{3AE}\right)_F + \left(\frac{a}{3AE}\right)_S - \frac{2b}{Gta}\right]_i - \left(\frac{2b^3}{3AE}\right)_{R,i-1}\left(\frac{1}{a_{i-1}} + \frac{1}{a_i}\right)\frac{1}{a_i} - \left(\frac{2b^3}{3AE}\right)_{R,i}\left(\frac{1}{a_i} + \frac{1}{a_{i+1}}\right)\frac{1}{a_i}$$

$$\omega_{i,i} = \left[\left(\frac{2a}{3AE}\right)_F + \left(\frac{2a}{3AE}\right)_S + \frac{2b}{Gta}\right]_i + \left[\left(\frac{2a}{3AE}\right)_F + \left(\frac{2a}{3AE}\right)_S + \frac{2b}{Gta}\right]_{i+1} + \left(\frac{2b^3}{3AE}\right)_{R,i-1}\left(\frac{1}{a_i}\right)^2 + \left(\frac{2b^3}{3AE}\right)_{R,i}\left(\frac{1}{a_i} + \frac{1}{a_{i+1}}\right)^2 + \left(\frac{2b^3}{3AE}\right)_{R,i+1}\left(\frac{1}{a_{i+1}}\right)^2$$

$$\omega_{i,i+1} = \left[\left(\frac{a}{3AE}\right)_F + \left(\frac{a}{3AE}\right)_S - \frac{2b}{Gta}\right]_i - \left(\frac{2b^3}{3AE}\right)_{R,i}\left(\frac{1}{a_i} + \frac{1}{a_{i+1}}\right)\frac{1}{a_{i+1}} - \left(\frac{2b^3}{3AE}\right)_{R,i+1}\left(\frac{1}{a_{i+1}} + \frac{1}{a_{i+2}}\right)\frac{1}{a_{i+1}}$$

$$\omega_{i,i+2} = \left(\frac{2b^3}{3AE}\right)_{R,i+1} \frac{1}{a_{i+1}} \frac{1}{a_{i+2}}$$

and

$$\lambda_i = \omega_{i,i-2}P_{i-2} + \left[\omega_{i,i-1} - \left(\frac{2a}{3AE}\right)_{F,i}\right]P_{i-1} +$$

$$\left[\omega_{i,i} - \left(\frac{4a}{3AE}\right)_{F,i} - \left(\frac{4a}{3AE}\right)_{F,i+1}\right]P_i + \left[\omega_{i,i+1} - \left(\frac{2a}{3AE}\right)_{F,i+1}\right]P_{i+1} +$$

$$\omega_{i,i+2}P_{i+2} - \left[(a\alpha T)_F - (a\alpha T)_S\right]_i - \left[(a\alpha T)_F - (a\alpha T)_S\right]_{i+1} -$$

$$\left[(b^2\alpha T)_{R,i-1}\frac{1}{a_i} - (b^2\alpha T)_{R,i}\left(\frac{1}{a_i} + \frac{1}{a_{i+1}}\right) + (b^2\alpha T)_{R,i+1}\frac{1}{a_{i+1}}\right]$$

The boundary equations are not listed since they depend on the particular end conditions of each problem. They can be easily obtained by minimizing the total energy with respect to the X-forces at the fixed boundaries or from the known forces at a free boundary.

APPENDIX D

FOUR-FLANGE BOX BEAM

Figure 13 illustrates the four-flange box that is analyzed. The assumptions made are that no external loads are applied to the beam, that the temperature distribution over the cross section is arbitrary, that the elastic properties of the material are independent of temperature, that the cross section is doubly symmetrical, and that the box beam has closely spaced rigid bulkheads.

Since the thermal stress system is self-equilibrating, it can be represented by the X-forces and shear flows q shown in figure 13. This system is the only possible self-equilibrating one in a four-flange box.

The equation of equilibrium for any one of the four corner flanges is

$$\frac{d}{dx}(X) + 2q = 0 \tag{D1}$$

The following stress-strain relations can be written

$$\left.\begin{aligned} \frac{X}{AE} &= \left(\frac{du}{dx} - \alpha T\right)_1 \\ &= -\left(\frac{du}{dx} - \alpha T\right)_2 \\ &= \left(\frac{du}{dx} - \alpha T\right)_3 \\ &= -\left(\frac{du}{dx} - \alpha T\right)_4 \end{aligned}\right\} \tag{D2}$$

$$\left.\begin{aligned} q &= Gt_c\left[\frac{1}{c}(u_4 - u_1) - \frac{dw}{dx} + \frac{b}{2}\frac{d\theta}{dx}\right] \\ &= Gt_b\left[\frac{1}{b}(u_2 - u_1) + \frac{dv}{dx} - \frac{c}{2}\frac{d\theta}{dx}\right] \\ &= Gt_c\left[\frac{1}{c}(u_2 - u_3) + \frac{dw}{dx} + \frac{b}{2}\frac{d\theta}{dx}\right] \\ &= Gt_b\left[\frac{1}{b}(u_4 - u_3) - \frac{dv}{dx} - \frac{c}{2}\frac{d\theta}{dx}\right] \end{aligned}\right\} \tag{D3}$$

and from equation (D3),

$$\frac{dv}{dx} = \frac{1}{2b}(u_1 - u_2 - u_3 + u_4) \tag{D4}$$

$$\frac{dw}{dx} = -\frac{1}{2c}(u_1 + u_2 - u_3 - u_4) \tag{D5}$$

$$\frac{d\theta}{dx} = \frac{1}{bc}\frac{\frac{b}{t_b} - \frac{c}{t_c}}{\frac{b}{t_b} + \frac{c}{t_c}}(u_1 - u_2 + u_3 - u_4) \tag{D6}$$

$$q = \frac{-G}{\frac{b}{t_b} + \frac{c}{t_c}}(u_1 - u_2 + u_3 - u_4) \tag{D7}$$

Differentiating equation (D1) with respect to x and substituting from equations (D2) and (D7) leads to the following differential equation:

$$\frac{d^2X}{dx^2} - K^2X = \frac{AE\alpha K^2}{4}(T_1 - T_2 + T_3 - T_4) \tag{D8}$$

where

$$K^2 = \frac{\frac{8G}{AE}}{\frac{b}{t_b} + \frac{c}{t_c}}$$

The solution of equation (D8) depends upon the manner in which the flange temperatures vary with x. Solutions are presented for three cases, in each of which the boundary conditions are that the X-forces are zero at the tip ($x = l$) and the shear flow is zero at the root ($x = 0$).

If the temperature is constant in the spanwise direction, the solution is

$$T_i = T_{i,o} \tag{D9}$$

$$X = -\frac{AE\alpha}{4}(T_1 - T_2 + T_3 - T_4)_o\left(1 - \frac{\cosh Kx}{\cosh Kl}\right) \tag{D10}$$

$$q = -\frac{KAE\alpha}{8}(T_1 - T_2 + T_3 - T_4)_o \frac{\sinh Kx}{\cosh Kl} \tag{D11}$$

$$v = \frac{ax^2}{4b}(T_1 - T_2 - T_3 + T_4)_o \tag{D12}$$

$$w = -\frac{ax^2}{4c}(T_1 + T_2 - T_3 - T_4)_o \tag{D13}$$

$$\theta = \frac{AE\alpha}{8Gbc}\left(\frac{b}{t_b} - \frac{c}{t_c}\right)(T_1 - T_2 + T_3 - T_4)_o \frac{\cosh Kx - 1}{\cosh Kl} \tag{D14}$$

If the temperature decreases linearly in the spanwise direction, the solution is

$$T_i = T_{i,o}\left(1 - \frac{x}{l}\right) \tag{D15}$$

$$X = -\frac{AE\alpha}{4}(T_1 - T_2 + T_3 - T_4)_o\left[1 - \frac{x}{l} - \frac{\sinh K(l - x)}{Kl \cosh Kl}\right] \tag{D16}$$

$$q = -\frac{AE\alpha}{8l}(T_1 - T_2 + T_3 - T_4)_o\left[1 - \frac{\cosh K(l - x)}{\cosh Kl}\right] \tag{D17}$$

$$v = \frac{\alpha x^2}{4b}(T_1 - T_2 - T_3 + T_4)_o\left(1 - \frac{x}{3l}\right) \tag{D18}$$

$$w = -\frac{\alpha x^2}{4c}(T_1 + T_2 - T_3 - T_4)_o\left(1 - \frac{x}{3l}\right) \tag{D19}$$

$$\theta = \frac{AE\alpha}{8Gbc}\left(\frac{b}{t_b} - \frac{c}{t_c}\right)(T_1 - T_2 + T_3 - T_4)_o\left[\frac{x}{l} + \frac{\sinh K(l - x) - \sinh Kl}{Kl \cosh Kl}\right] \tag{D20}$$

If the temperature increases linearly in the spanwise direction, the solution is

$$T_i = T_{i,o}\frac{x}{l} \tag{D21}$$

$$X = -\frac{AE\alpha}{4}(T_1 - T_2 + T_3 - T_4)_o\left[\frac{x}{l} - \frac{\cosh Kx}{\cosh Kl} + \frac{\sinh K(l - x)}{Kl \cosh Kl}\right] \quad (D22)$$

$$q = \frac{AE\alpha}{8l}(T_1 - T_2 + T_3 - T_4)_o\left[1 - \frac{Kl \sinh Kx + \cosh K(l - x)}{\cosh Kl}\right] \quad (D23)$$

$$v = \frac{\alpha x^3}{12bl}(T_1 - T_2 - T_3 + T_4)_o \quad (D24)$$

$$w = -\frac{\alpha x^3}{12cl}(T_1 + T_2 - T_3 - T_4)_o \quad (D25)$$

$$\theta = -\frac{AE\alpha}{8Gbc}\left(\frac{b}{t_b} - \frac{c}{t_c}\right)(T_1 - T_2 + T_3 - T_4)_o\left[\frac{x}{l} - \frac{\cosh Kx - 1}{\cosh Kl} + \frac{\sinh K(l - x) - \sinh Kl}{Kl \cosh Kl}\right] \quad (D26)$$

APPENDIX E

ELEMENTARY METHOD OF ANALYSIS

The detailed procedures commonly used for aircraft structural analysis take a variety of forms, but they are all based on ordinary shell theory, which is a simple extension of beam theory. In this appendix the procedure of reference 15 is modified to permit the calculation of elementary temperature effects. The sign conventions and rotation of figure 14 are used.

Bending Stresses

In accordance with the assumption that plane cross sections remain plane, the strain at any point can be written as a linear function of the coordinates as follows:

$$\epsilon_j = \frac{1}{E_o}\left(k_1 y_j + k_2 z_j + k_3\right) \tag{E1}$$

If the elastic properties are regarded as functions of temperature, the stress at a point is

$$\sigma_j = E_j(\epsilon - \alpha T)_j$$

$$= \frac{E_j}{E_o}\left(k_1 y_j + k_2 z_j + k_3\right) - (E\alpha T)_j \tag{E2}$$

Expressions for k can be obtained from the equilibrium equations of the cross section which require that

$$\sum_j (\sigma A)_j = 0 \tag{E3a}$$

$$\sum_j (\sigma A z)_j = M_y \tag{E3b}$$

$$\sum_j (\sigma A y)_j = -M_z \tag{E3c}$$

Substituting equation (E2) into (E3) yields

$$k_1 \sum_j \left(\frac{AEy}{E_o}\right)_j + k_2 \sum_j \left(\frac{AEz}{E_o}\right)_j + k_3 \sum_j \left(\frac{AE}{E_o}\right)_j - \sum_j (AE\alpha T)_j = 0 \qquad (E4a)$$

$$k_1 \sum_j \left(\frac{AEyz}{E_o}\right)_j + k_2 \sum_j \left(\frac{AEz^2}{E_o}\right)_j + k_3 \sum_j \left(\frac{AEz}{E_o}\right)_j - \sum_j (AE\alpha Tz)_j = M_y \qquad (E4b)$$

$$k_1 \sum_j \left(\frac{AEy^2}{E_o}\right)_j + k_2 \sum_j \left(\frac{AEyz}{E_o}\right)_j + k_3 \sum_j \left(\frac{AEy}{E_o}\right)_j - \sum_j (AE\alpha Ty)_j = -M_z \qquad (E4c)$$

The resulting expressions for k_1, k_2, and k_3 can be greatly simplified by the proper choice of coordinate axes, the greatest simplification being achieved by the use of a set of effective principal axes of inertia. However, since principal axes are often inconvenient to use, the following formulas are presented for any set of arbitrary orthogonal axes:

$$k_1 = \frac{I_{yy}(N_z - M_z) - I_{yz}(N_y + M_y)}{I_{yy}I_{zz} - I_{yz}^2} \qquad (E5a)$$

$$k_2 = \frac{I_{zz}(N_y + M_y) - I_{yz}(N_z - M_z)}{I_{yy}I_{zz} - I_{yz}^2} \qquad (E5b)$$

$$k_3 = -k_1\bar{y} - k_2\bar{z} + \frac{\sum_j (AE\alpha T)_j}{\sum_j (\eta A)_j} \qquad (E5c)$$

where the effectiveness factor η_j is

$$\eta_j = \frac{E_j}{E_o}$$

the coordinates of effective centroid are

$$\bar{y} = \frac{\sum_j (\eta A y)_j}{\sum_j (\eta A)_j}$$

$$\bar{z} = \frac{\sum_j (\eta A z)_j}{\sum_j (\eta A)_j}$$

the effective moments of inertia are

$$I_{yy} = \sum_j (\eta A z^2)_j - \bar{y} \sum_j (\eta A z)_j$$

$$I_{zz} = \sum_j (\eta A y^2)_j - \bar{y} \sum_j (\eta A y)_j$$

$$I_{yz} = \sum_j (\eta A y z)_j - \bar{y} \sum_j (\eta A z)_j$$

and the effective moments of thermal expansion are

$$N_y = \sum_j (AE\alpha T z)_j - \bar{z} \sum_j (AE\alpha T)_j$$

$$N_z = \sum_j (AE\alpha T y)_j - \bar{y} \sum_j (AE\alpha T)_j$$

Shear Stresses

The shear flow in a given panel can be determined from the bending stresses as follows:

$$q_j = q_{j-1} + \frac{\Delta(\sigma A)_j}{\Delta x} \qquad \text{(E6)}$$

Equation (E6) is sufficient to define completely the shear flow in an open-section beam since the shear flow is zero at the boundaries. A single-cell beam is still statically determinate, however, and the following additional equilibrium equation that relates the internal shear flows to the applied torque may be written:

$$\sum_j (mq)_j = -M_x \tag{E7}$$

where

$$m_j = z_j y_{j+1} - z_{j+1} y_j$$

A multicell beam is statically indeterminate, and additional equations are required. These equations may be obtained from the requirement of equal twist of all cells and the following equation for the angle of twist of a cell:

$$2A\theta = \sum_j \left(\frac{qb}{Gt}\right)_j \tag{E8}$$

where A is the area enclosed by the cell and the summation is taken around the cell. In evaluating equation (E8) it should be remembered that the modulus of rigidity G is a function of temperature.

APPENDIX F

APPROXIMATING THE END EFFECT

The secondary thermal stresses near a stress-free end can be approximately determined by applying a self-equilibrating force group to the end of the structure to liquidate the elementary stresses and so satisfy the boundary conditions for stress. The rate of decay of this force group is determined by a minimum-energy principle. The problem is made as simple as possible by assuming that the temperature distribution over a cross section does not vary along the length of the beam and that the beam contains closely spaced rigid bulkheads. The notations and sign conventions of figure 14 apply.

The force in any stringer is assumed to be the product of a function of the cross section times a function of x

$$(\sigma A)_{x,j} = (\sigma A)_j \varphi(x) \tag{F1}$$

The distribution of $(\sigma A)_j$ is given by the elementary analysis (appendix E).

The shear flow around the section is

$$q_{x,j} = q_j \frac{d}{dx}\left[\varphi(x)\right] \tag{F2}$$

where q_j is the shear flow determined from an elementary analysis in which the assumption is made that

$$\frac{\Delta(\sigma A)_{x,j}}{\Delta x} = (\sigma A)_j \tag{F3}$$

The decay function $\varphi(x)$ can be determined from the principle of minimum complementary energy. The total strain energy can be expressed in terms of φ as follows:

$$U = \frac{1}{2}\sum_j \left(\frac{\sigma^2 A}{E}\right)_j \int_0^l \varphi^2 dx + \frac{1}{2}\sum_j \left(\frac{q^2 b}{Gt}\right)_j \int_0^l \left(\frac{d\varphi}{dx}\right)^2 dx \tag{F4}$$

The variation of the strain energy is then determined and set equal to zero; the result is

$$\delta U = \int_0^l \left[\varphi \sum_j \left(\frac{\sigma^2 A}{E} \right)_j - \frac{d^2\varphi}{dx^2} \sum_j \left(\frac{q^2 b}{Gt} \right)_j \right] \delta\varphi \, dx + \sum_j \left(\frac{q^2 b}{Gt} \right)_j \left[\frac{d\varphi}{dx} \delta\varphi \right]_0^l = 0 \qquad (F5)$$

The strain energy is a minimum if φ satisfies the following differential equation:

$$\frac{d^2\varphi}{dx^2} - K^2\varphi = 0 \qquad (F6)$$

where

$$K^2 = \frac{\sum_j \left(\frac{\sigma^2 A}{E} \right)_j}{\sum_j \left(\frac{q^2 b}{Gt} \right)_j}$$

With the coordinate system of figure 14 and a beam of length l, the following solution of the differential equations satisfies the boundary conditions of $\frac{d\varphi}{dx} = 0$ when $x = 0$ and $\varphi = 1$ when $x = l$:

$$\varphi = \frac{\cosh Kx}{\cosh Kl} \qquad (F7)$$

A more convenient form of solution is that for an infinitely long beam in which x is measured from the end at which the force group is applied; then

$$\varphi = e^{-Kx} \qquad (F8)$$

Equation (F7) is similar to those previously obtained for the simple panel (appendix B) since this method gives the exact solution to problems that involve only one statically indeterminate force group. In general, the distribution over the cross section varies with x and it is possible for a solution obtained by this method to contain appreciable errors. However, it does yield a reasonable approximation with a small expenditure of effort.

REFERENCES

1. Lo, Hsu: Determination of Transient Skin Temperature of Conical Bodies during Short-Time, High-Speed Flight. NACA TN 1725, 1948.

2. Huston, Wilber B., Warfield, Calvin N., and Stone, Anna Z.: A Study of Skin Temperatures of Conical Bodies in Supersonic Flight. NACA TN 1724, 1948.

3. Tendeland, Thorval, and Schlaff, Bernard A.: Temperature Gradients in the Wing of a High-Speed Airplane during Dives from High Altitudes. NACA TN 1675, 1948.

4. Stalder, Jackson R., and Jukoff, David: Heat Transfer to Bodies Traveling at High Speed in the Upper Atmosphere. NACA Rep. 944, 1949.

5. Johnson, H. A., Rubesin, M. W., Sauer, F. M., Slack, E. G., and Possner, L.: A Design Manual for Determining the Thermal Characteristics of High Speed Aircraft. AAF TR No. 5632, Air Materiel Command, Army Air Forces, Sept. 10, 1947.

6. Holms, Arthur G., and Faldetta, Richard D.: Effects of Temperature Distribution and Elastic Properties of Materials on Gas-Turbine-Disk Stresses. NACA Rep. 864, 1947.

7. Timoshenko, S.: Theory of Elasticity. First ed., McGraw-Hill Book Co., Inc., 1934.

8. Goodier, J. N.: Thermal Stresses. Jour. Appl. Mech., vol. 4, no. 1, March 1937, pp. A-33 - A-36.

9. Jones, Alun R., and Schlaff, Bernard A.: An Investigation of a Thermal Ice-Prevention System for a C-46 Cargo Airplane. VII - Effect of the Thermal System on the Wing-Structure Stresses as Established in Flight. NACA ARR 5G20, 1945.

10. Heldenfels, Richard R.: A Numerical Method for the Stress Analysis of Stiffened-Shell Structures under Nonuniform Temperature Distributions. NACA TN 2241, 1950.

11. Heimerl, George J., and Roberts, William M.: Determination of Plate Compressive Strengths at Elevated Temperatures. NACA Rep. 960, 1950.

12. Hodgman, Charles D., ed.: Handbook of Chemistry and Physics. Twenty-eighth ed., Chemical Rubber Publishing Co., 1944.

13. Kuhn, Paul, and Chiarito, Patrick T.: Shear Lag in Box Beams - Methods of Analysis and Experimental Investigations. NACA Rep. 739, 1942.

14. Ebner, H., and Köller, H.: Über den Kraftverlauf in längs- und querversteiften Scheiben. Luftfahrtforschung, Bd. 15, Lfg. 10/11, Oct. 10, 1938, pp. 527-542.

15. Bruhn, E. F.: Analysis and Design of Airplane Structures. Fifth printing, Tri-State Offset Co. (Cincinnati, Ohio), 1943.

TABLE I.- NUMERICAL ANALYSIS OF A WING SECTION

(a) Section Properties

①	②	③	④	⑤	⑥	⑦	⑧	⑨	⑩	⑪	⑫	⑬	⑭	⑮	⑯	⑰	⑱
j	A	y	z	T	E	α	$E\alpha T$	$AE\alpha T$	$AE\alpha Ty$	$AE\alpha Tz$	η	ηA	ηAy	ηAz	ηAy^2	ηAz^2	ηAyz
							⑤×⑥×⑦	②×⑧	③×⑨	④×⑨	⑥/10.5	②×⑫	③×⑬	④×⑬	③×⑭	④×⑮	④×⑭
1a	2.35	-40.00	0	225	9.4048×10^6	13.312×10^{-6}	28,169.26	66,197.76	-2,647,910.4	0	0.895695	2.104883	-84.19532	0	3,367.8128	0	0
1b	2.35	-40.00	0	250	9.1888	13.400	30,782.48	72,338.83	-2,893,553.2	0	.875124	2.056541	-82.26164	0	3,290.4656	0	0
2a	2.35	-15.00	3.75	175	9.7803	13.136	22,482.95	52,834.93	-792,524.0	198,130.99	.931457	2.188924	-32.83386	8.208465	492.5079	30.78174	-123.1270
2b	2.35	-15.00	3.75	125	10.0803	12.960	16,330.09	38,375.71	-575,635.6	143,908.91	.960029	2.256068	-33.84102	8.460255	507.6153	31.72596	-126.9038
2c	1.00	-15.00	3.75	75	10.3048	12.784	9,880.24	9,880.24	-148,203.6	37,050.90	.981410	.981410	-14.72115	3.680288	220.8173	13.80108	-55.2043
3	.30	-15.00	.75	50	10.3888	12.696	6,594.81	1,978.44	-29,676.6	1,483.83	.989410	.296823	-4.45235	.222617	66.7852	16696	-3.3393
4a	1.00	-15.00	-2.25	100	10.2020	12.872	13,132.01	13,132.01	-196,980.2	-29,547.02	.971619	.971619	-14.57429	-2.186143	218.6144	4.91882	32.7922
4b	2.35	-15.00	-2.25	200	9.6020	13.224	25,395.37	59,679.12	-895,186.8	-134,278.02	.914476	2.149019	-32.23529	-4.835293	483.5294	10.87941	72.5294
4c	2.35	-15.00	-2.25	150	9.9398	13.048	19,454.18	45,717.32	-685,759.8	102,863.97	.946648	2.224623	-33.36935	-5.005402	500.5403	11.26215	75.0810
5a	2.35	10.00	5.00	100	10.2020	12.872	13,132.01	30,860.22	308,602.2	154,301.10	.971619	2.283305	22.83305	11.416525	228.3305	57.08265	114.1653
5b	2.35	10.00	5.00	125	10.0803	12.960	16,330.09	38,375.71	383,757.1	191,878.55	.960029	2.256068	22.56068	11.280340	225.6068	56.40170	112.8034
5c	1.00	10.00	5.00	50	10.3888	12.696	6,594.81	6,594.81	65,948.1	32,974.05	.989410	.989410	9.89410	4.947050	98.9410	24.73525	49.4705
6	.45	10.00	1.00	25	10.4538	12.608	3,295.04	1,482.77	14,827.7	1,482.77	.995600	.448020	4.48020	448020	44.8020	.44802	4.4802
7a	1.00	10.00	-3.00	75	10.3048	12.784	9,880.24	9,880.24	98,802.4	-29,640.72	.981410	.981410	9.81410	-2.944230	98.1410	8.83269	-29.4423
7b	2.35	10.00	-3.00	125	10.0803	12.960	16,330.09	38,375.71	383,757.1	-115,127.13	.960029	2.256068	22.56068	-6.768204	225.6068	20.30461	-67.6820
7c	2.35	10.00	-3.00	150	9.9398	13.048	19,454.18	45,717.32	457,173.2	-137,151.96	.946648	2.224623	22.24623	-6.673869	222.4623	20.02161	-66.7387
8a	2.35	35.00	3.75	150	9.9398	13.048	19,454.18	45,717.32	1,600,106.2	171,439.95	.946648	2.224623	77.86181	8.342336	2,725.1632	31.28376	291.9818
8b	1.00	35.00	3.75	75	10.3048	12.784	9,880.24	9,880.24	345,808.4	37,050.90	.981410	.981410	34.34935	3.680288	1,202.2273	13.80108	128.8101
9	.30	35.00	.75	50	10.3888	12.696	6,594.81	1,978.44	69,245.4	1,483.83	.989410	.296823	10.38881	.222617	363.6084	16696	7.7916
10a	1.00	35.00	-2.25	100	10.2020	12.872	13,132.01	13,132.01	459,620.3	-29,547.02	.971619	.971619	34.00667	-2.186143	1,190.2335	4.91882	-76.5150
10b	2.35	35.00	-2.25	150	9.9398	13.048	19,454.18	45,717.32	1,600,106.2	-102,863.97	.946648	2.224623	77.86181	-5.005402	2,725.1634	11.26215	-175.1891
$\sum$	35.25							647,846.47	-3,077,675.8	290,165.97		33.367912	16.37322	25.304115	18,498.9744	352.79542	165.7640

NACA

Stresses due to external load:

$M_y = -4 \times 10^6$

$M_z = -1 \times 10^6$

$k_1 = -M_z C_1 - M_y C_3 = 154.104$

$k_2 = M_y C_2 + M_z C_3 = -12{,}061.022$

$k_3 = -k_1 \bar{y} - k_2 \bar{z} = 9{,}070.701$

Stresses due to temperature:

$N_y = \sum ⑪ - \bar{z} \sum ⑨ = -3{,}395{,}566$

$N_z = \sum ⑩ - \bar{y} \sum ⑨ = -201{,}120$

$k_1 = N_z C_1 - N_y C_3 = -179.318$

$k_2 = N_y C_2 - N_z C_3 = -520.440$

$k_3 = \frac{\sum ⑨}{\sum ⑬} - k_1 \bar{y} - k_2 \bar{z} = 19{,}897.911$

where

$\bar{y} = \frac{\sum ⑭}{\sum ⑬} = 0.490688$

$\bar{z} = \frac{\sum ⑮}{\sum ⑬} = 0.758337$

$I_{yy} = \sum ⑰ - \bar{z} \sum ⑮ = 333.606$

$I_{zz} = \sum ⑯ - \bar{y} \sum ⑭ = 18{,}490.941$

$I_{yz} = \sum ⑱ - \bar{y} \sum ⑮ = 153.348$

$C_0 = \frac{10^6}{I_{yy} I_{zz} - I_{yz}^2} = 0.162729$

$10^6 C_1 = I_{yy} C_0 = 54.2875$

$10^6 C_2 = I_{zz} C_0 = 3{,}009.0169$

$10^6 C_3 = I_{yz} C_0 = 24.9541$

TABLE I.- NUMERICAL ANALYSIS OF A WING SECTION - Continued

(b) Bending stresses and axial loads.

⑲	⑳	㉑	㉒	㉓	㉔	㉕	㉖	㉗
j	σ_L	$(\sigma A)_L$	σ_T	$(\sigma A)_T$	σ	σA	σ for $T_j = 0$	σA for $T_j = 0$
	*	②× ⑳	**	②× ㉒	⑳ + ㉒	㉑ + ㉓		②× ㉖
1a	2,603	6,118	-3,922	-9,217	-1,319	-3,099	2,509	5,895
1b	2,544	5,977	-7,092	-16,667	-4,548	-10,690	2,509	5,895
2a	-35,833	-84,207	-3,261	-7,664	-39,094	-91,871	-37,056	-87,082
2b	-36,932	-86,790	3,481	8,181	-33,451	-78,609	-37,056	-87,082
2c	-37,755	-37,755	10,372	10,372	-27,383	-27,383	-37,056	-37,056
3	-2,262	-679	15,367	4,610	13,105	3,931	-2,421	-726
4a	32,934	32,934	9,952	9,952	42,886	42,886	32,214	32,214
4b	30,997	72,844	-3,669	-8,621	27,328	64,223	32,214	75,702
4c	32,088	75,407	3,037	7,137	35,125	82,544	32,214	75,702
5a	-48,283	-113,465	1,931	4,537	-46,352	-108,928	-47,759	-112,233
5b	-47,707	-112,112	-1,447	-3,401	-49,154	-115,513	-47,759	-112,233
5c	-49,167	-49,167	8,744	8,744	-40,423	-40,423	-47,759	-47,759
6	-1,443	-649	14,212	6,395	12,769	5,746	-1,579	-711
7a	45,925	45,925	9,420	9,420	55,345	55,345	44,601	44,601
7b	44,924	105,572	2,550	5,992	47,474	111,564	44,601	104,812
7c	44,298	104,101	-837	-1,967	43,461	102,134	44,601	104,812
8a	-29,123	-68,439	-8,407	-19,756	-37,530	-88,195	-29,599	-69,558
8b	-30,193	-30,193	1,573	1,573	-28,620	-28,620	-29,599	-29,599
9	5,361	1,608	6,497	1,949	11,858	3,557	5,036	1,511
10a	40,421	40,421	1,241	1,241	41,662	41,662	39,671	39,671
10b	39,382	92,548	-5,451	-12,809	33,931	79,739	39,671	93,226
$\sum$		-1		1		0		2

*$(\sigma_L)_j = ⑫\left(k_1 \times ③ + k_2 \times ④ + k_3\right)_L$

**$(\sigma_T)_j = ⑫\left(k_1 \times ③ + k_2 \times ④ + k_3\right)_T - ⑧$

TABLE I.- NUMERICAL ANALYSIS OF A WING SECTION - Continued

(c) Shear stresses.

(28)	(29)	(30)	(31)	(32)	(33)	(34)	(35)	(36)	(37)	(38)	(39)	(40)	(41)	(42)	(43)	(44)	(45)	(46)	(47)	(48)	(49)	(50)	(51)
Stringer	y	z	$\frac{\Delta(\sigma A)}{\Delta x}$	Panel	q	m	mq	T	G	b	t	b/Gt	b/Gt	b/Gt	qb/Gt	qb/Gt	qb/Gt	q_1	q_2	q_3	q	τ	τ for $T_j = 0$
						***	(33) × (34)					Cell 1	Cell 2	Cell 3	Cell 1	Cell 2	Cell 3				(33) + (46) + (47) + (48)	(49)/(38)	
--	------	-----	---------	4-1	0	90.0	0	225.0	3.4330×10^{6}	25.1010	0.188	38.89193×10^{-6}	----------	----------	0 $\times10^{-6}$	----------	----------	-1,644.24	-------	---------	-1,644.24	-8,748	-9,398
1	-40.00	0	-193.53	1-2	-193.53	150.0	-29,029.5	200.0	3.5200	25.2797	.188	38.20071	----------	----------	-7,392.98	----------	----------	-1,644.24	-------	---------	-1,837.77	-9,775	-10,402
2	-15.00	3.75	3,340.03	2-3	3,146.50	-45.0	-141,592.5	62.5	3.8913	3.0000	.081	9.51802	9.51802×10^{-6}	----------	29,948.45	$29,948.45\times10^{-6}$	----------	-1,644.24	2,126.22	---------	3,628.48	44,796	43,610
3	-15.00	.75	10.86	3-4	3,157.36	-45.0	-142,081.2	75.0	3.8650	3.0000	.081	9.58266	9.58266	----------	30,255.91	30,255.91	----------	-1,644.24	2,126.22	---------	3,639.34	44,930	43,753
4	-15.00	-2.25	-2,898.96	4-7	258.40	-67.5	-17,442.0	137.5	3.7113	25.0112	.188	----------	35.84730	----------	----------	9,262.94	----------	--------	2,126.22	---------	2,384.62	12,684	12,622
7	10.00	-3.00	-4,089.57	7-6	-3,831.17	-40.0	153,246.8	50.0	3.9610	4.0000	.081	----------	12.46723	12.46723×10^{-6}	----------	-47,764.08	$-47,764.08\times10^{-6}$	--------	2,126.22	-1,467.64	-3,172.59	-39,168	-38,331
6	10.00	1.00	10.39	6-5	-3,820.78	-40.0	152,831.2	37.5	3.9813	4.0000	.081	----------	12.40382	12.40382	----------	-47,392.27	-47,392.27	--------	2,126.22	-1,467.64	-3,162.20	-39,040	-38,191
--	------	-----	---------	5-2	0	-112.5	0	112.5	3.7773	25.0312	.188	----------	35.24910	----------	----------	0	----------	--------	2,126.22	---------	2,126.22	11,310	11,215
5	10.00	5.00	4,395.90	5-8	575.12	137.5	79,079.0	137.5	3.7113	25.0312	.188	----------	----------	35.87597	----------	----------	20,632.99	--------	--------	-1,467.64	-892.52	-4,747	-4,501
8	35.00	3.75	1,578.11	8-9	2,153.23	105.0	226,089.2	62.5	3.8913	3.0000	.081	----------	----------	9.51802	----------	----------	20,494.49	--------	--------	-1,467.64	685.59	8,464	9,140
9	35.00	.75	-25.73	9-10	2,127.50	105.0	223,387.5	75.0	3.8650	3.0000	.081	----------	----------	9.58266	----------	----------	20,387.11	--------	--------	-1,467.64	659.86	8,146	8,841
10	35.00	-2.25	-2,127.50	10-7	0	82.5	0	150.0	3.6780	25.0112	.188	----------	----------	36.19105	----------	----------	0	--------	--------	-1,467.64	-1,467.64	-7,807	-7,501
$\sum$							504,488.5					96.19332×10^{-6}	115.06813×10^{-6}	116.03875×10^{-6}	$52,811.38\times10^{-6}$	$-25,689.05\times10^{-6}$	$-33,641.76\times10^{-6}$						

***$m = z_j y_{j+1} \quad z_{j+1} y_j$

Moment equation:

$$1 \times 10^{6} = 504,488.5 + 150q_1 \quad 350q_2 + 350q_3$$

Twist equations:

Cell 1 $150\theta = \left(52,811.38 + 96.19332q_1 + 19.10068q_2\right) \times 10^{-6}$

Cell 2 $-350\theta = \left(-25,689.05 + 19.10068q_1 + 115.06813q_2 + 24.87105q_3\right) \times 10^{-6}$

Cell 3 $350\theta = \left(-33,641.76 + 24.87105q_2 + 116.03875q_3\right) \times 10^{-6}$

TABLE I.- NUMERICAL ANALYSIS OF A WING SECTION - Concluded

(d) Approximate determination of the end effect.

(52)	(53)
j	$\frac{\sigma_T^2 A}{\eta}$
	(23)²/(13)
1a	40.360 × 10⁶
1b	135.076
2a	26.834
2b	29.666
2c	109.616
3	71.599
4a	101.935
4b	34.584
4c	22.833
5a	9.015
5b	5.127
5c	77.276
6	91.282
7a	90.417
7b	15.914
7c	1.741
8a	175.445
8b	2.521
9	12.798
10a	1.585
10b	73.752
Σ	1,129.376

(54)	(55)	(56)	(57)	(58)	(59)	(60)	(61)	(62)	(63)	(64)	(65)	(66)	(67)
$\frac{\Delta(\sigma A)}{\Delta x}$	Panel	q	mq	qb/Gt	qb/Gt	qb/Gt	q_1	q_2	q_3	q	$\frac{q^2 b}{Gt}$	q_{max}	τ_{max}
			(34) × (56)	Cell 1	Cell 2	Cell 3				(56)+(61)+(62)+(63)	(64)² × (41)	K × (64)	(66)/(39)
--------	4-1	0	0	0	----------	----------	-13,251	---	------	-13,251	6,829.0	-825.9	-4,393
25,884	1-2	25,884	3,882,600	988,787 × 10⁻⁶	----------	----------	-13,251	---	------	12,633	6,096.6	787.4	4,188
-10,889	2-3	14,995	-674,775	142,723	142,723 × 10⁻⁶	----------	-13,251	586	------	2,330	51.7	145.2	1,793
-4,610	3-4	10,385	-467,325	99,516	99,516	----------	-13,251	586	------	-2,280	49.8	-142.1	-1,754
-8,468	4-7	1,917	-129,398	----------	68,719	----------	-------	586	------	2,503	224.6	156.0	830
-13,445	7-6	-11,528	461,120	----------	-143,722	-143,722 × 10⁻⁶	-------	586	12,717	1,775	39.3	110.6	1,366
-6,395	6-5	-17,923	716,920	----------	-222,314	-222,314	-------	586	12,717	-4,620	264.8	-287.9	-3,555
-------	5-2	0	0	----------	0	----------	-------	586	------	586	12.1	36.5	194
-9,879	5-8	-27,802	-3,822,775	----------	----------	-997,424	-------	---	12,717	-15,085	8,163.8	-940.2	-5,001
18,183	8-9	-9,619	-1,009,995	----------	----------	-81,554	-------	---	12,717	3,098	91.4	193.1	2,384
-1,949	9-10	-11,568	-1,214,640	----------	----------	-110,852	-------	---	12,717	1,149	12.7	71.6	884
11,568	10-7	0	0	----------	----------	0	-------	---	12,717	12,717	5,852.9	792.6	4,216
Σ			-2,258,268	1,231,026 × 10⁻⁶	-55,078 × 10⁻⁶	-1,565,866 × 10⁻⁶					27,688.7		

(68)	(69)	(70)
x from tip	Kx	e^{-Kx}
0	0	1.000
10	.62	.538
20	1.24	.289
30	1.87	.154
40	2.59	.075
50	3.12	.044
60	3.74	.024
70	4.36	.013
80	4.98	.007
90	5.61	.004
100	6.23	002

NACA

Moment equation:

$$0 = -2{,}258{,}268 + 150q_1 - 350q_2 + 350q_3$$

Twist equations:

Cell 1 $\quad 150\theta = \left(1{,}231{,}026 + 96.19332q_1 + 19.10068q_2\right) \times 10^{-6}$

Cell 2 $\quad -350\theta = \left(-55{,}078 + 19.10068q_1 + 115.06813q_2 + 24.87105q_3\right) \times 10^{-6}$

Cell 3 $\quad 350\theta = \left(-1{,}565{,}866 + 24.87105q_2 + 116.03875q_3\right) \times 10^{-6}$

$$\sum_j \left(\frac{\sigma^2 A}{E}\right)_j = \frac{1129.376}{10.5} = 107.556$$

$$K^2 = \frac{107.556}{27{,}688.7} = 0.00388447$$

$$K = 0.062326$$

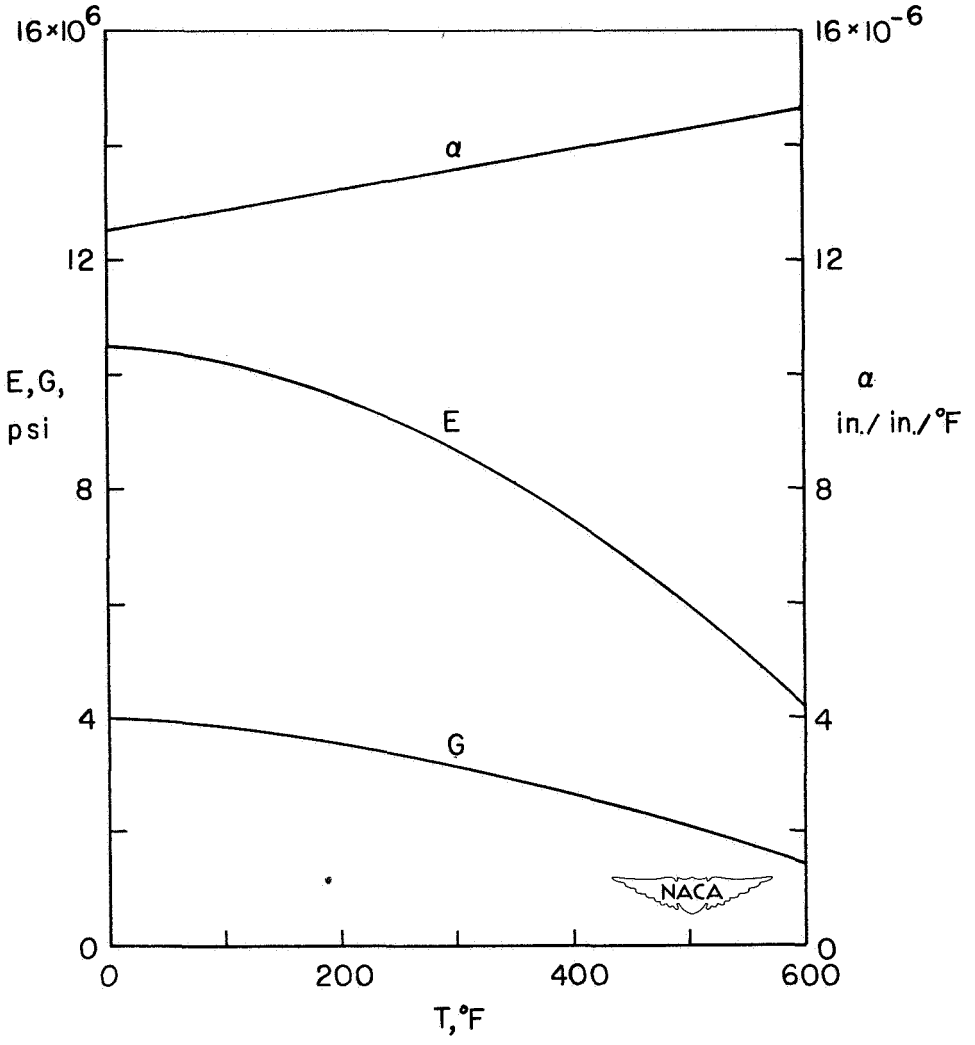

Figure 1.- Variation of elastic properties of 75S-T6 aluminum alloy with temperature increase as given empirically by

$\alpha = (12.52 + 0.00352T) \times 10^{-6}$ (Reference 12)

$E = (10.5 - 0.00147T - 0.0000151T^2) \times 10^6$ (Reference 11)

$G = (4.0 - 0.00144T - 0.0000048T^2) \times 10^6$ (Reference 11)

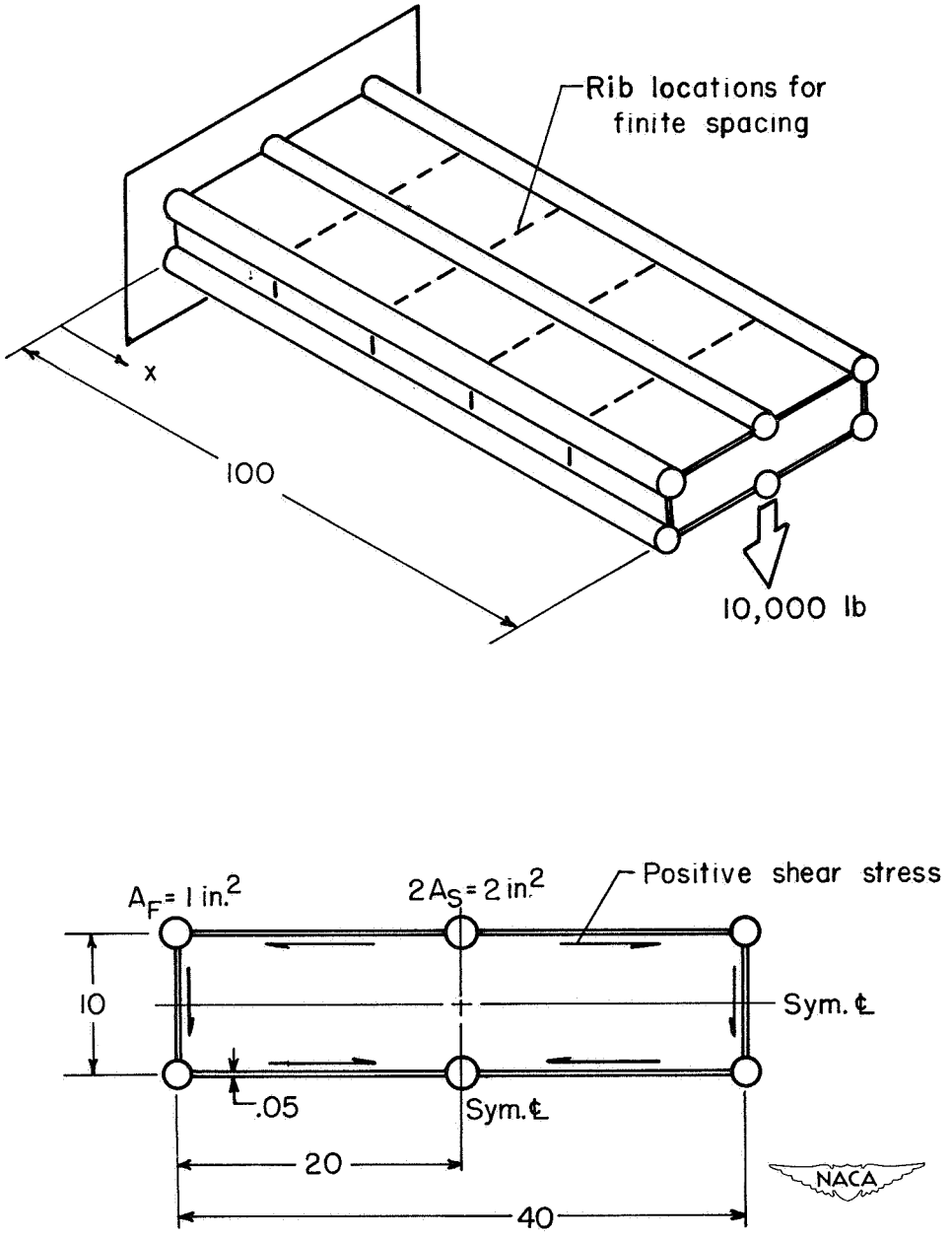

Figure 2.- Box beam used for stress-distribution examples.

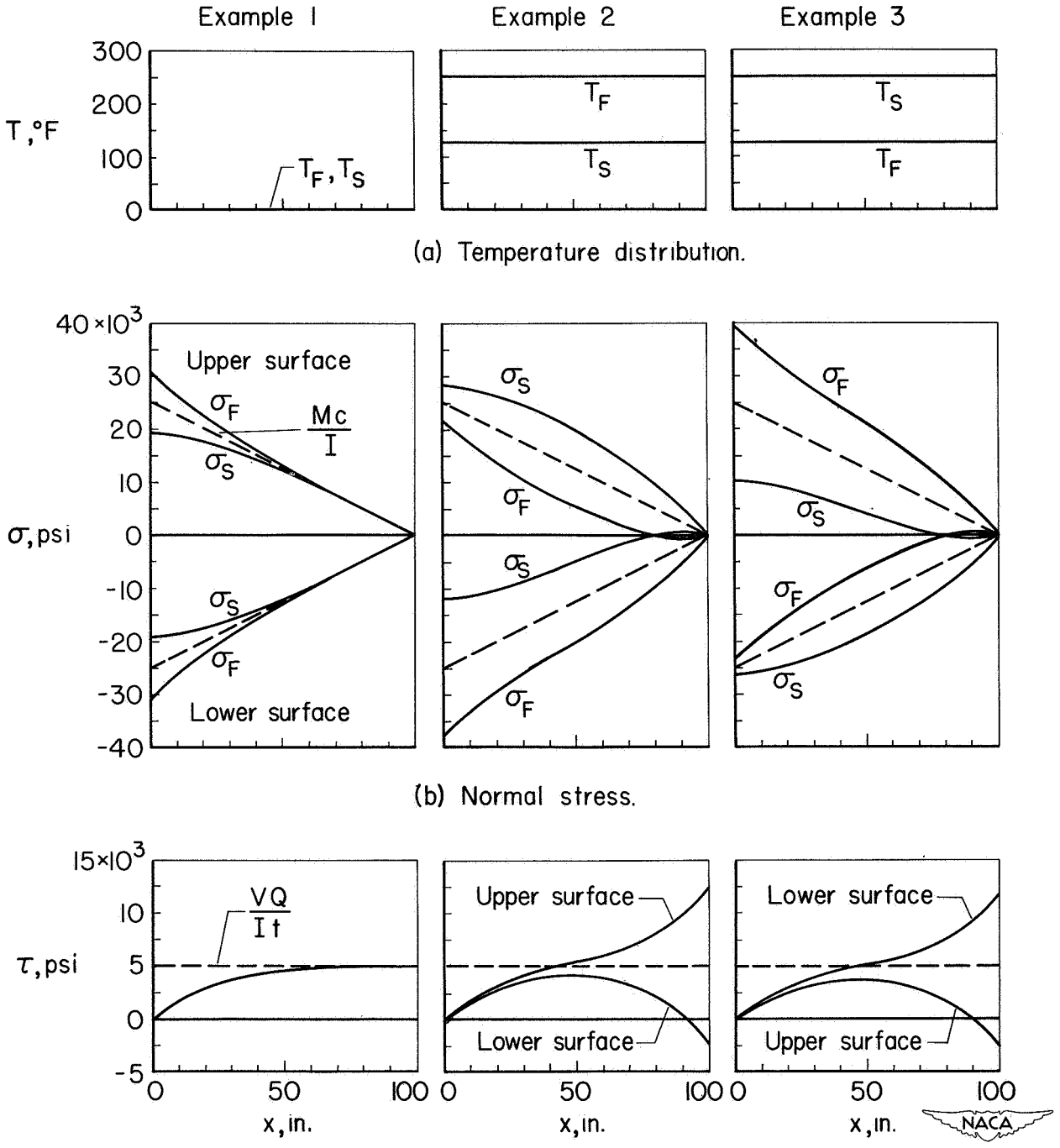

Figure 3.- Stress distribution in the box beam of figure 2 for three temperature distributions.

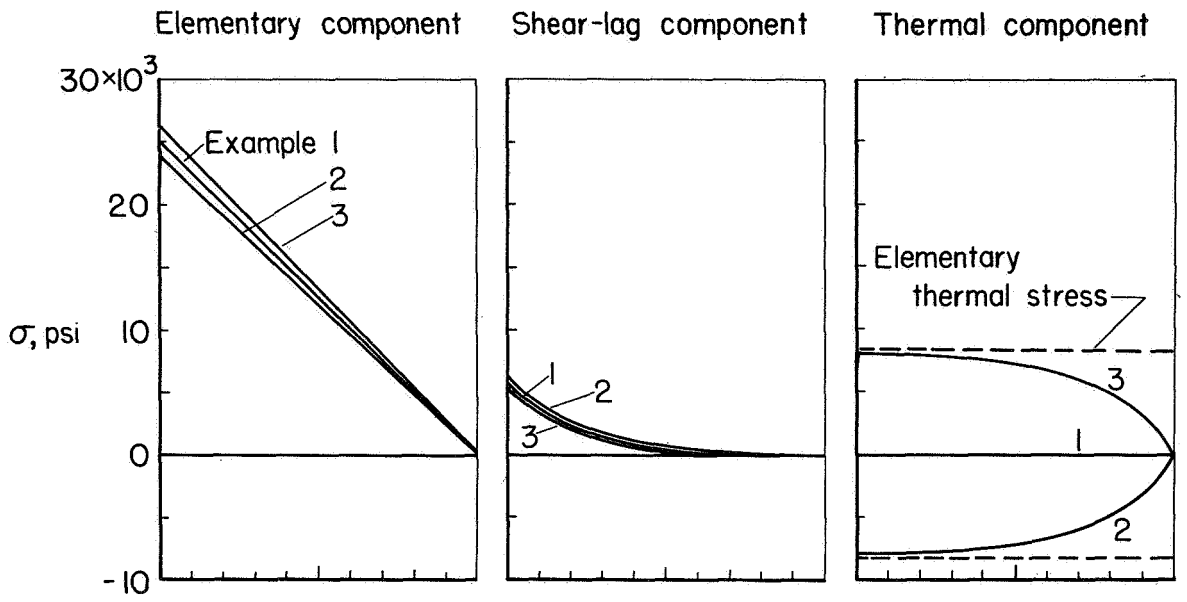

(a) Normal stress in upper flanges.

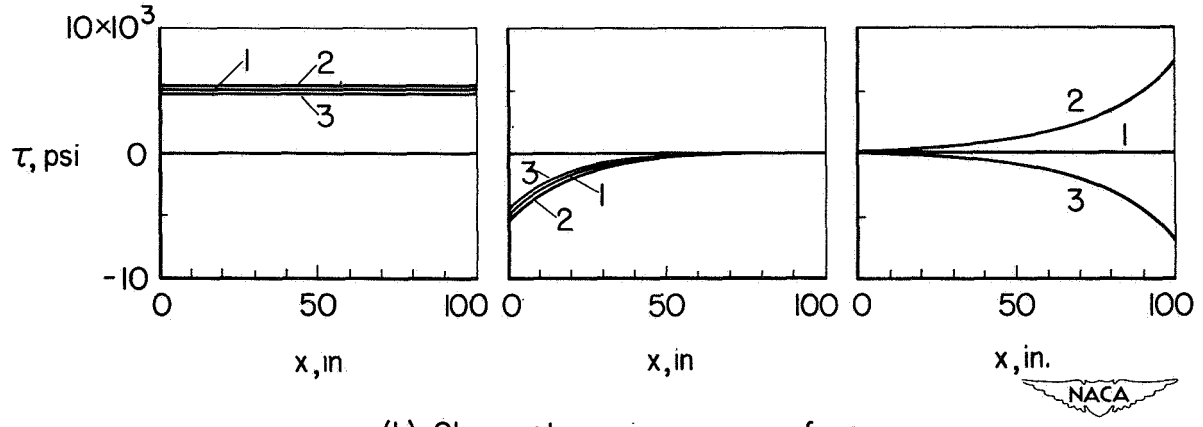

(b) Shear stress in upper surface.

Figure 4.- Stress components for the three examples given in figure 3.

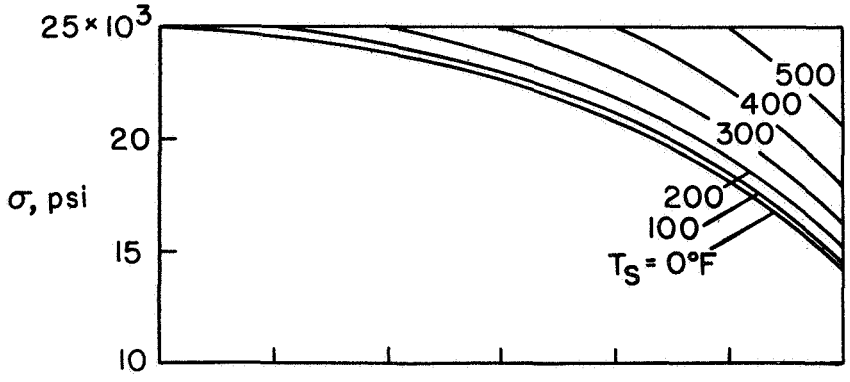

(a) Elementary bending stress.

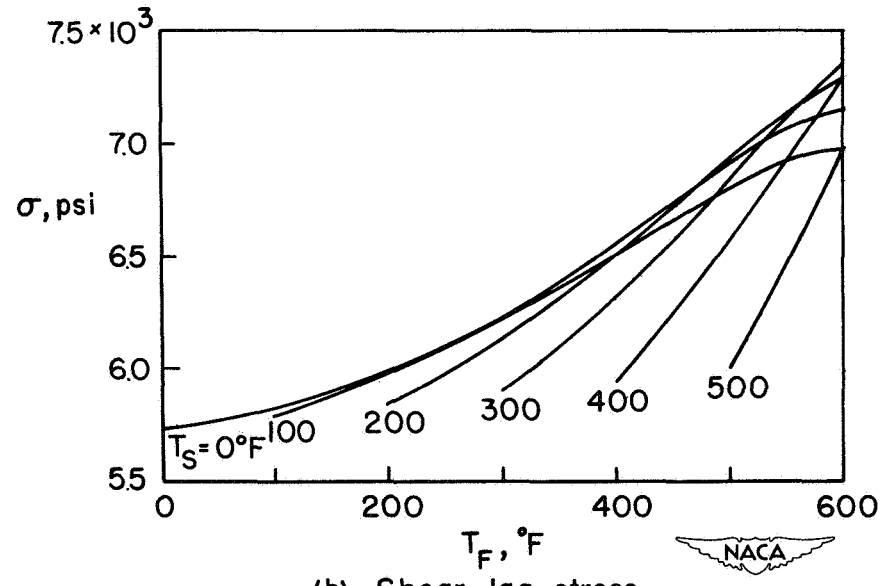

(b) Shear-lag stress.

Figure 5.- Effect of variable elastic properties on the stress in the upper flanges at x = 0.

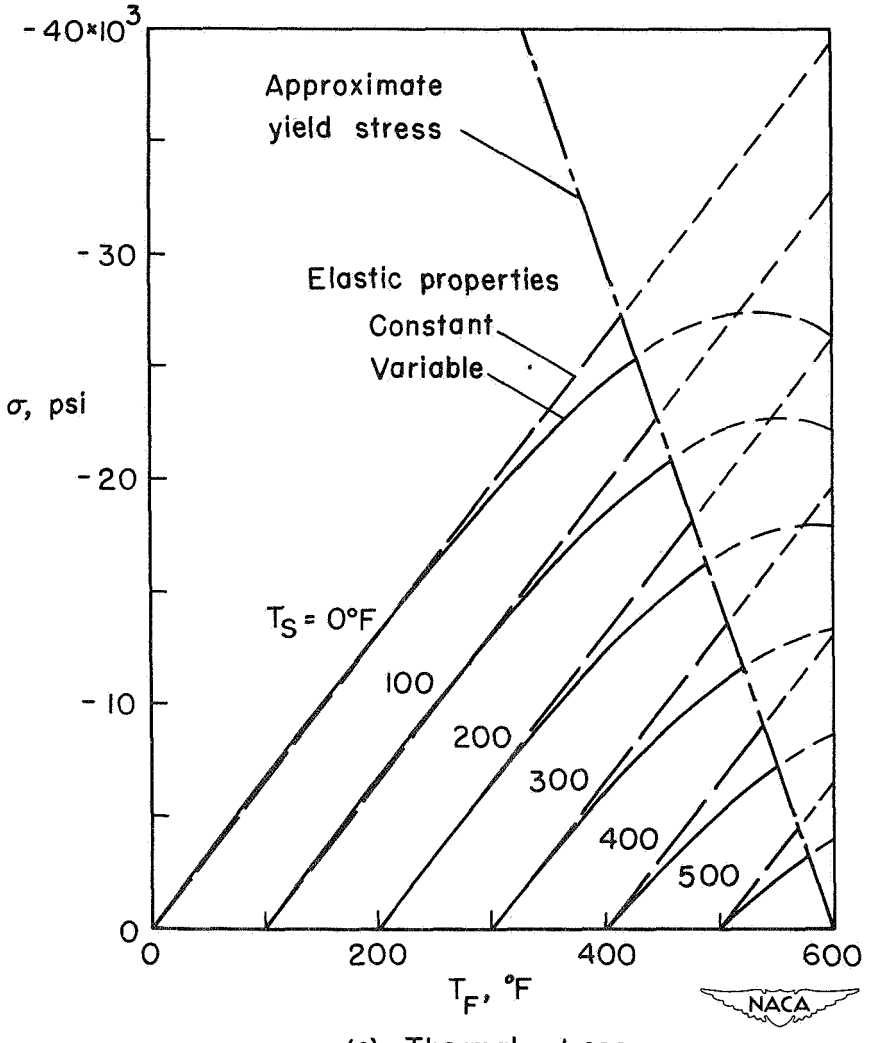

(c) Thermal stress.

Figure 5.- Concluded.

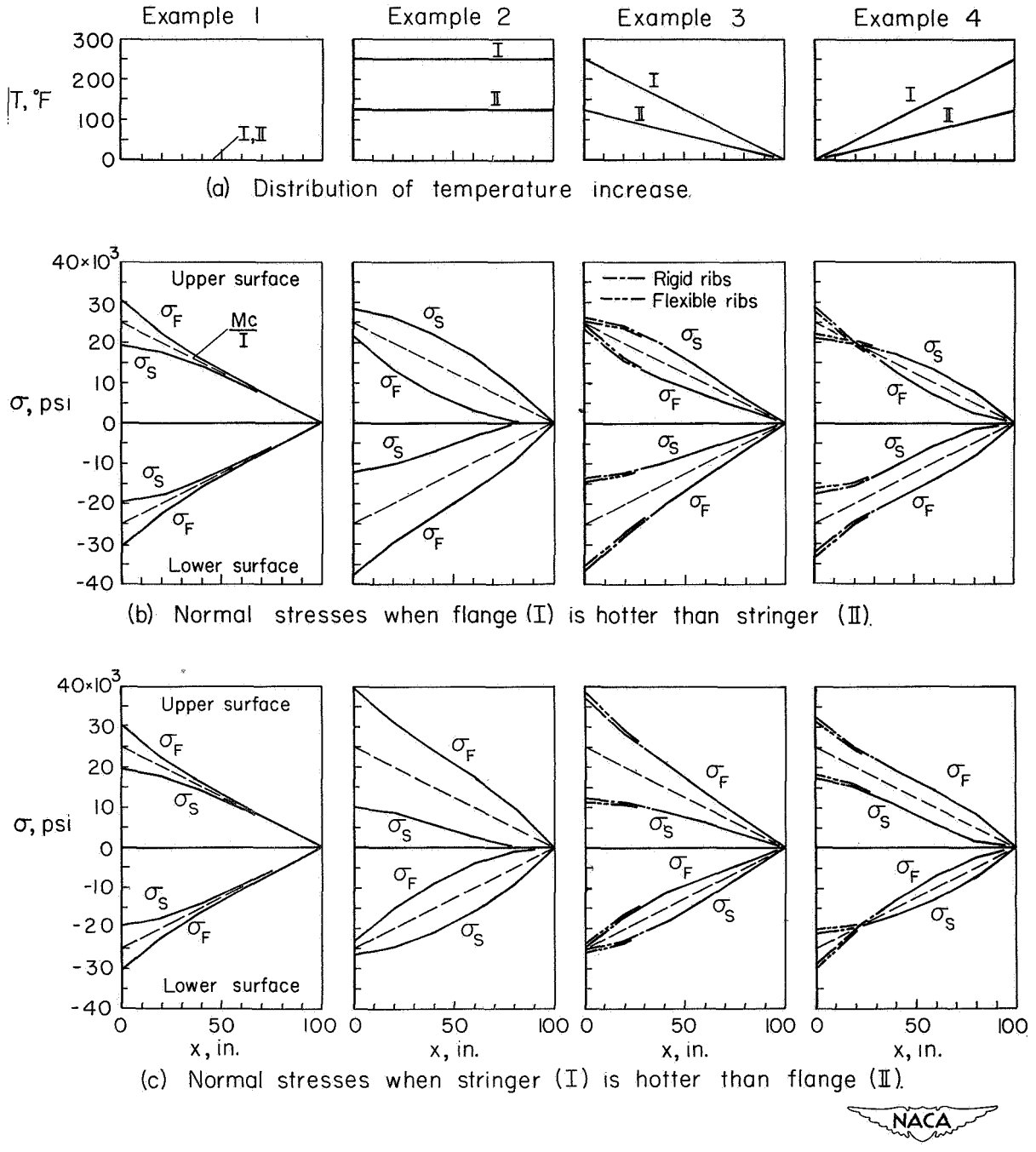

Figure 6.- Effects of rib stiffness on the stress distribution.

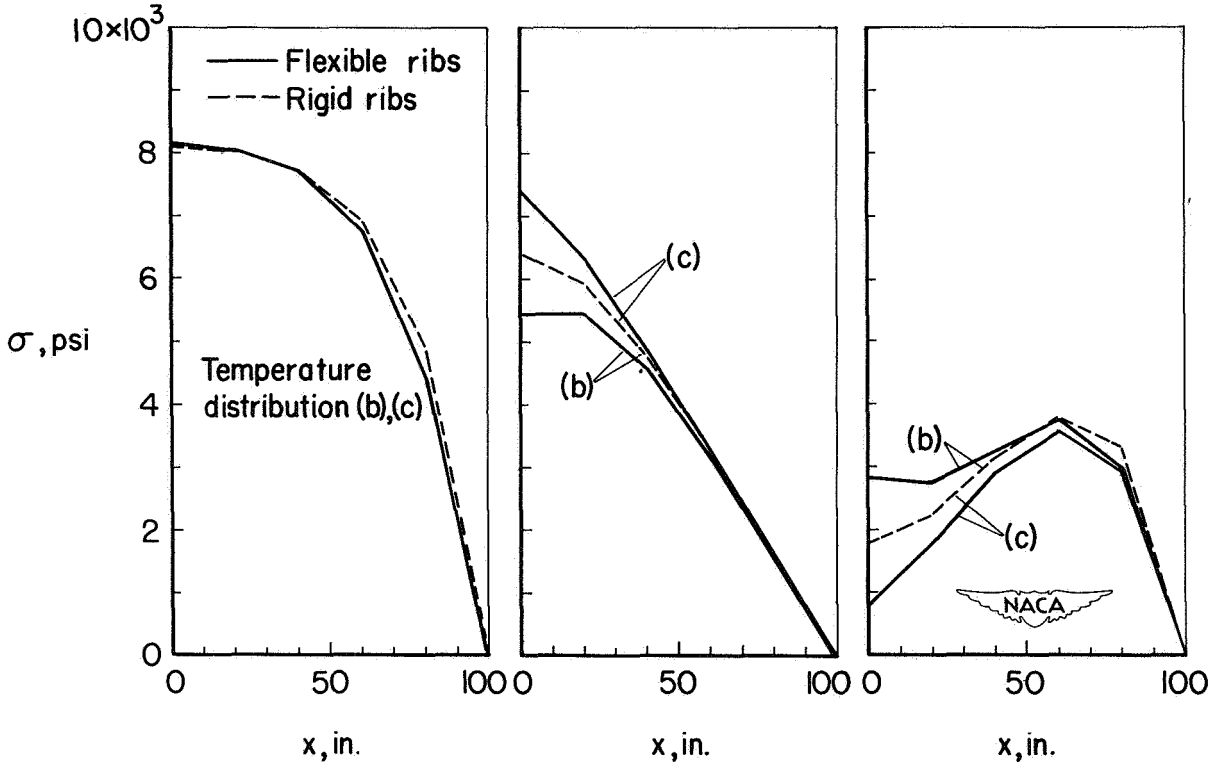

(a) Example 2. (b) Example 3. (c) Example 4.

Figure 7.- Thermal stress components for examples in figure 6.

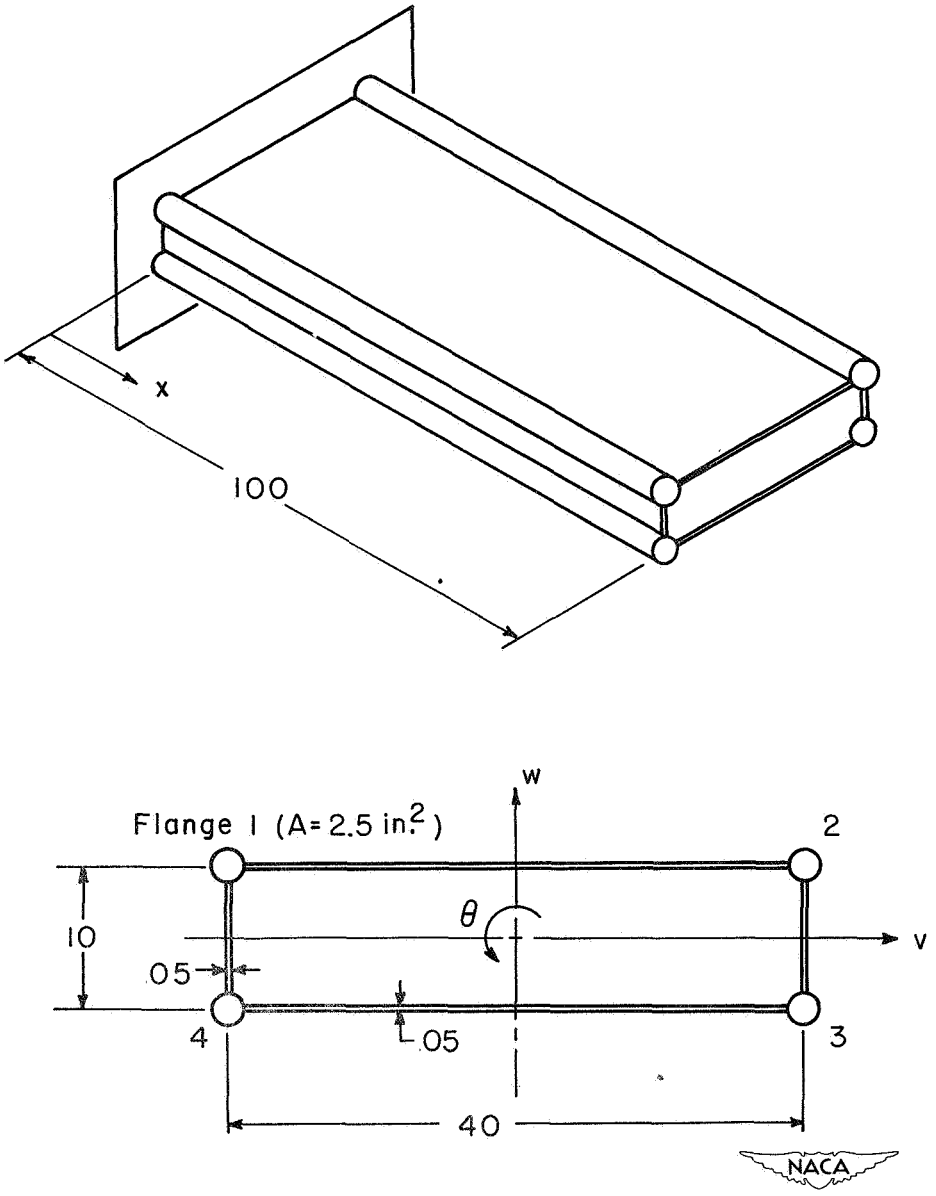

Figure 8.- Box beam used for examples of thermal distortions.

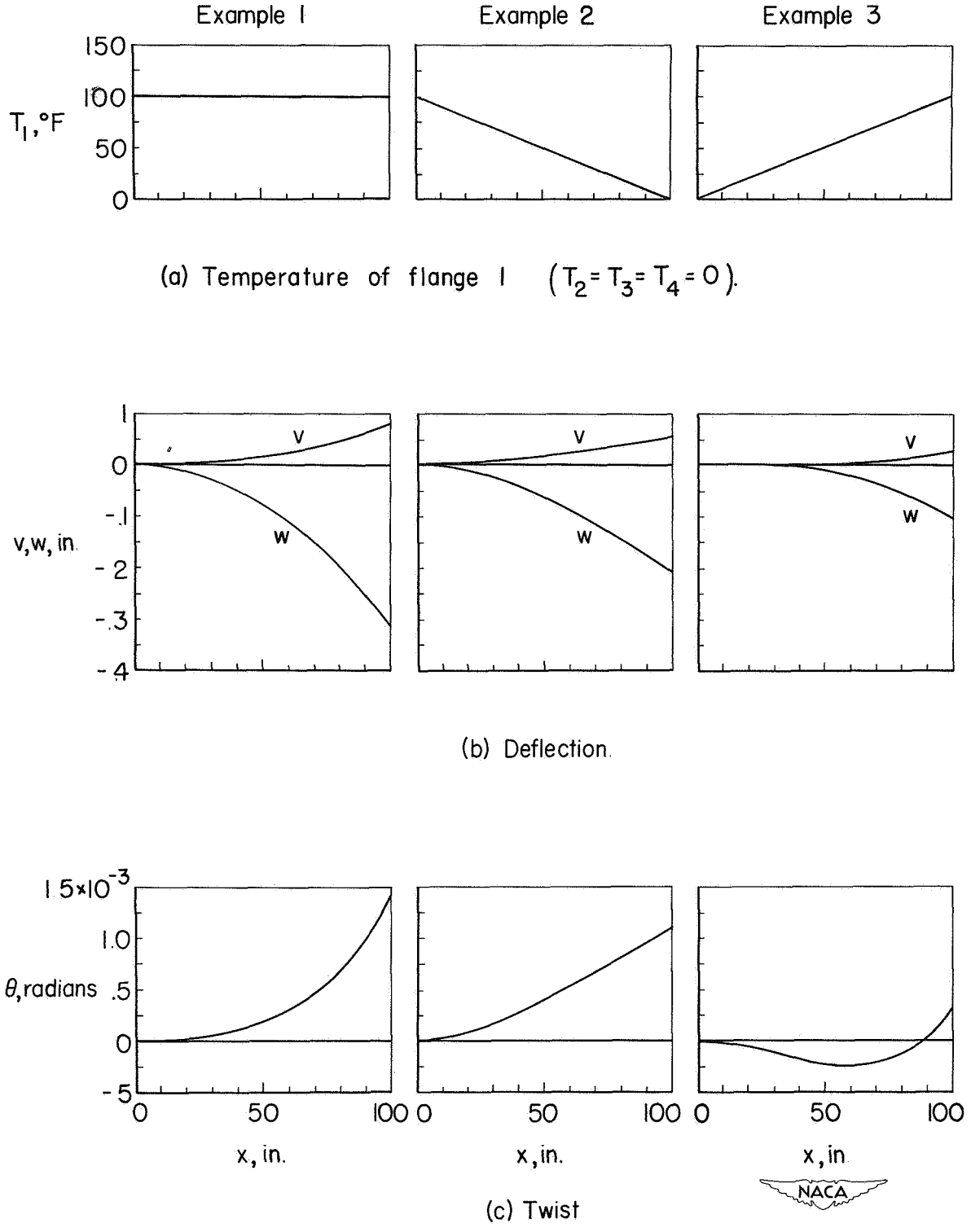

Figure 9.- Temperature distribution and thermal distortions of the four-flange box beam of figure 8.

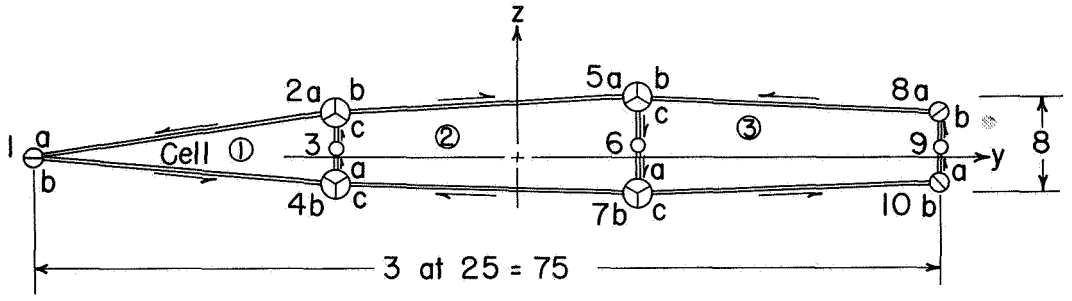

(a) Idealized wing section and positive direction of shear flows.

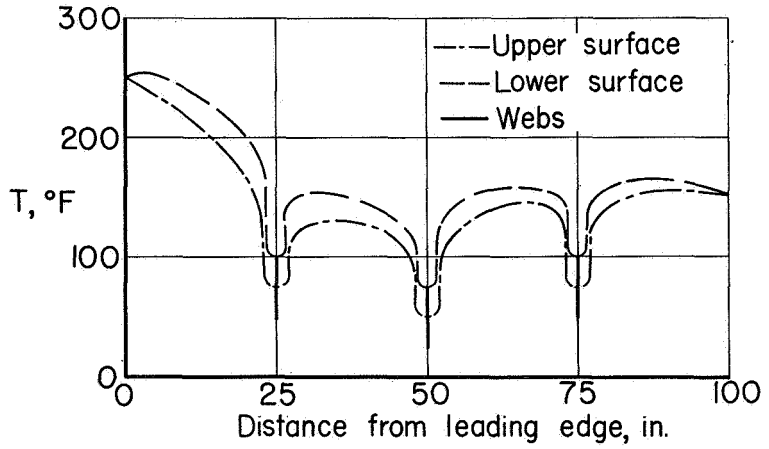

(b) Distribution of temperature increase.

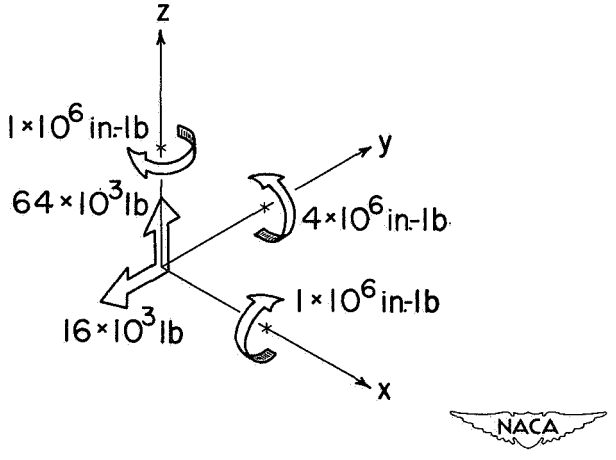

(c) Applied loads.

Figure 10.- Structure, temperatures, and loads used in example of elementary analysis.

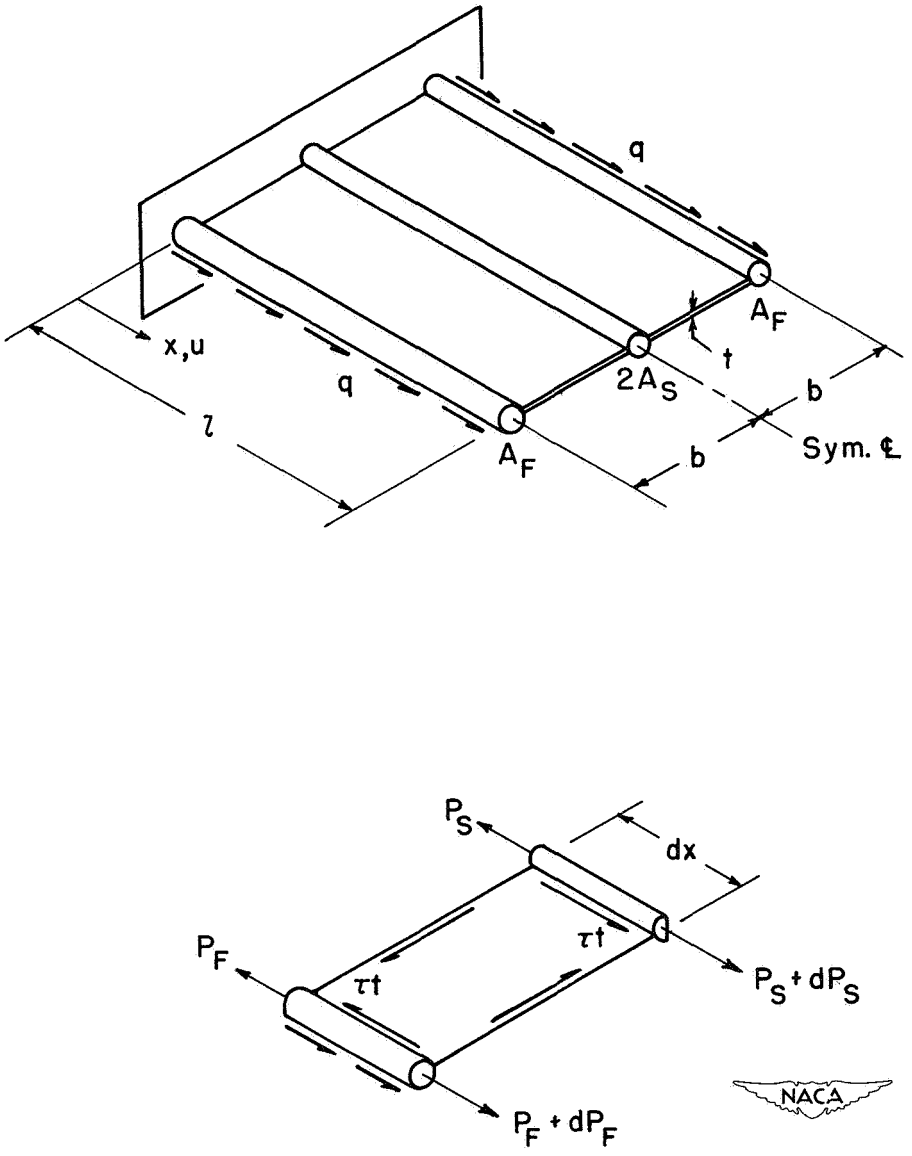

Figure 11.- Sign conventions and notation used in the analysis of the three-stringer panel with closely spaced rigid ribs (appendix B).

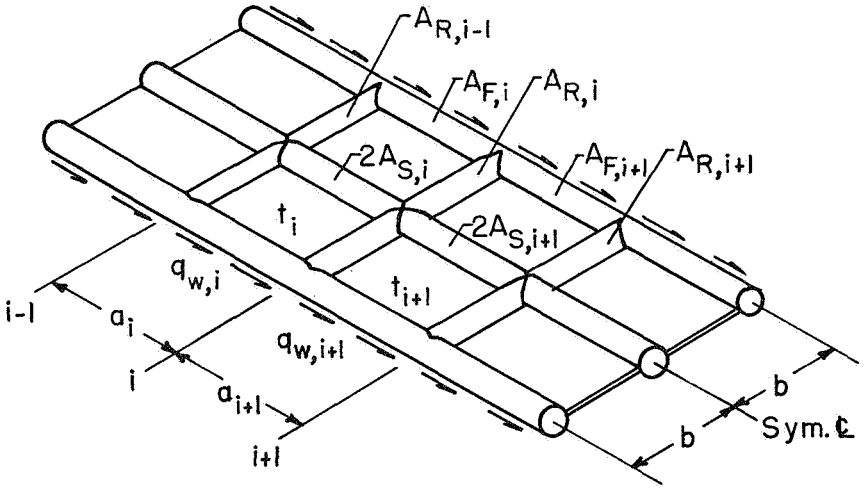

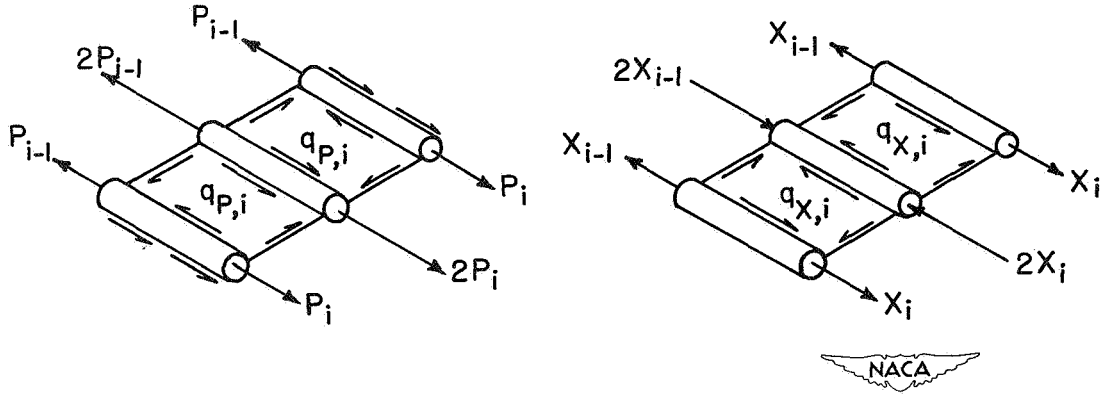

Figure 12.- Sign conventions and notation used in the analysis of the three-stringer panel with individual flexible ribs (appendix C).

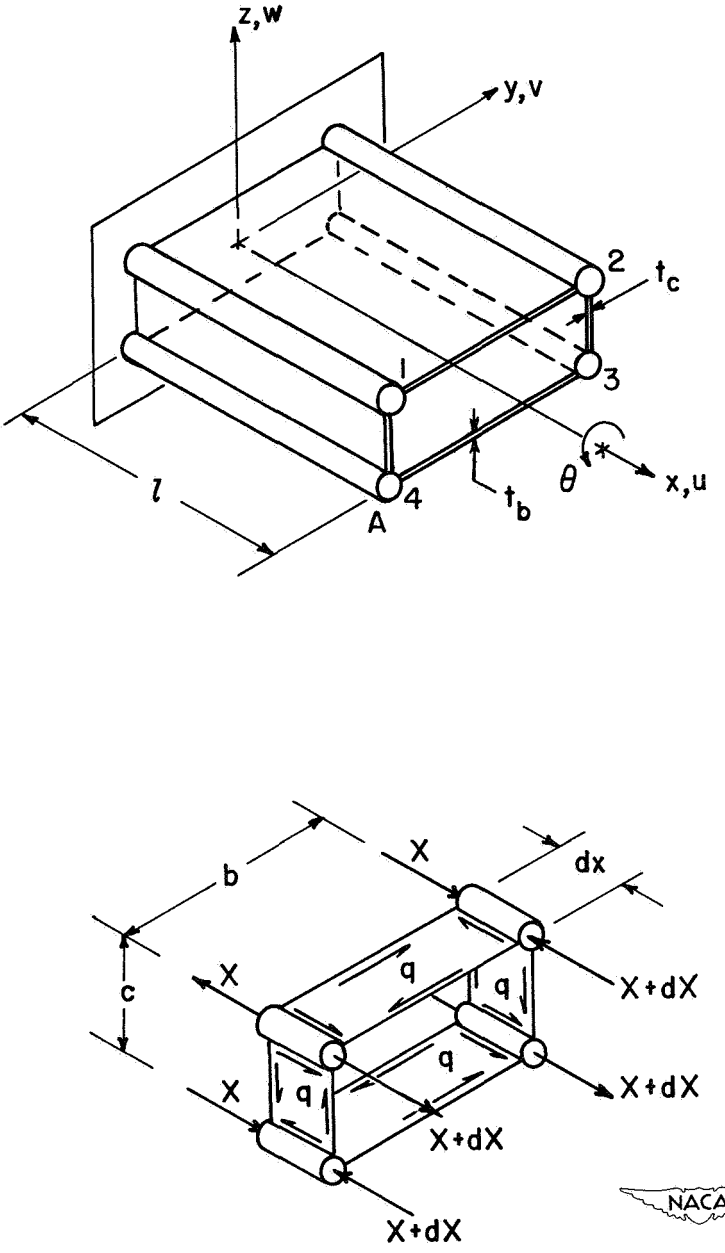

Figure 13.- Sign conventions and notation used in the four-flange box analysis (appendix D).

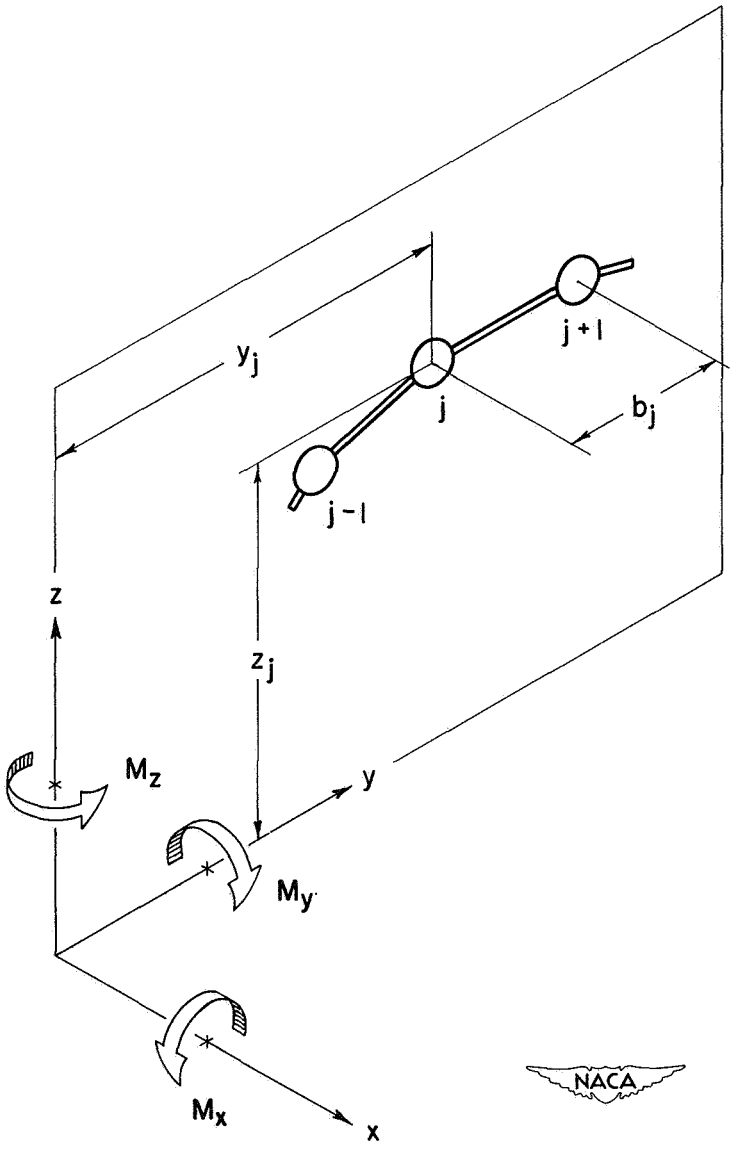

Figure 14.- Sign conventions and notations used in the elementary analysis (appendix E).